Journal Pre-proofs

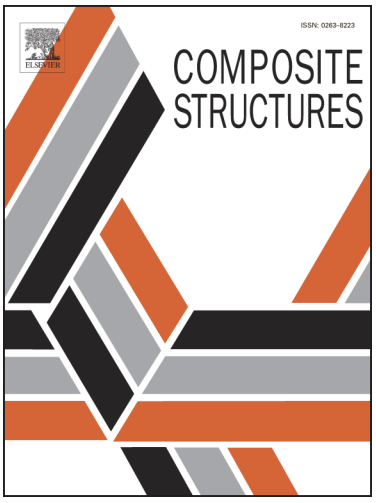

On the wave propagation of the multi-scale hybrid nanocomposite doubly curved viscoelastic panel

M.S.H. Al-Furjan, Mohammad Amin Oyarhossein, Mostafa Habibi, Hamed Safarpour, Dong Won Jung, Abdelouahed Tounsi

PII: S0263-8223(20)32873-7
DOI: https://doi.org/10.1016/j.compstruct.2020.112947
Reference: COST 112947

To appear in: *Composite Structures*

Received Date: 1 June 2020
Revised Date: 31 August 2020
Accepted Date: 9 September 2020

Please cite this article as: Al-Furjan, M.S.H., Amin Oyarhossein, M., Habibi, M., Safarpour, H., Won Jung, D., Tounsi, A., On the wave propagation of the multi-scale hybrid nanocomposite doubly curved viscoelastic panel, *Composite Structures* (2020), doi: https://doi.org/10.1016/j.compstruct.2020.112947

On the wave propagation of the multi-scale hybrid nanocomposite doubly curved viscoelastic panel

M.S.H. Al-Furjan[1,2] (Rayan@hdu.edu.cn)

Mohammad Amin Oyarhossein[3] (M.amin.oyarhossein@ua.pt)

Mostafa Habibi[4,5] (mostafahabibi@duytan.edu.vn) (*Corresponding Author)

Hamed Safarpour[6] (Hamed_safarpor@yahoo.com)

Dong Won Jung[7] (jdwcheju@jejunu.ac.kr) (*Corresponding Author)

Abdelouahed Tounsi [8] (tou_abdel@yahoo.com) (*Corresponding Author)

1. School of Mechanical Engineering, Hangzhou Dianzi University, Hangzhou 310018, China.
2. School of Materials Science and Engineering, State Key Laboratory of Silicon Materials, Zhejiang University, Hangzhou 310027, China.
3. Department of Civil Engineering, University of Aveiro, Aveiro, Portugal.
4. Institute of Research and Development, Duy Tan University, Da Nang, 550000, Vietnam.
5. Faculty of Electrical–Electronic Engineering, Duy Tan University, Da Nang, 550000, Vietnam.
6. Faculty of Engineering, Department of Mechanics, Imam Khomeini International University, Qazvin, Iran.
7. School of Mechanical Engineering, Jeju National University, Jeju, Jeju-do, 690-756, South Korea
8. Material and Hydrology Laboratory, University of Sidi Bel Abbes, Faculty of Technology, Civil Engineering Department, Algeria

Abstract:

In this paper, wave propagation analysis of multi-hybrid nanocomposite (MHC) reinforced doubly curved panel embedded in the viscoelastic foundation is carried out. Higher-order shear deformable theory (HSDT) is utilized to express the displacement kinematics. The rule of mixture and modified Halpin–Tsai model are engaged to provide the effective material constant of the MHC reinforced doubly curved panel. By employing Hamilton's principle, the governing equations of the structure are derived and solved with the aid of an analytical method. Afterward, a parametric study is carried out to investigate the effects of the viscoelastic foundation, carbon nanotubes' (CNTs') weight fraction, various MHC patterns, radius to total thickness ratio, and carbon fibers angel on the phase velocity of the MHC reinforced doubly curved panel in the viscoelastic medium. The results show that, by considering the viscous parameter, the relation between wavenumber and phase velocity changes from exponential increase to logarithmic boost. A useful suggestion of this research is that the effects of fiber angel and damping parameter on the phase velocity of a doubly curved panel are hardly dependent on the wavenumber. The presented study outputs can be used in ultrasonic inspection techniques and structural health monitoring.

Keywords:

MHC reinforcement, Doubly curved panel, Wave propagation, Fiber angle, Phase velocity, HSDT.

Introduction:

Nowadays, a lot of researches are presented to show the importance of composite materials and structures [1] because of that, these structures encounter us with an attractive property [2-6]. Based on the mentioned issue, static and dynamic stability of the composite structures become an important field of study[7, 8]. Also, structural health monitoring in the inhomogeneous structure is an essential issue that wave propagation responses are the main point of this filed [9-14].

In the field of frequency information of different structures, Mehar et al. [15-17] investigated thermal frequency of the graded nanotube-reinforced composite structure embedded with shape memory alloy fiber using a micromechanical multiscale finite element material model. They formulated the smart nanotube-reinforced composite structure through the higher-order kinematics, including the shear deformations. Katariya et al. [18] computed time-dependent deflection responses of the mechanically excited layered skew sandwich shell panels using the higher-order shear deformation theory, including the effects of the large displacement. Mehar et al. [19] investigated the free vibration behavior of functionally graded carbon nanotube-reinforced composite plate under an elevated thermal environment. They modeled carbon nanotube-reinforced composite plate mathematically using higher-order shear deformation theory. Sahu et al. [20] revealed the effect of hybridization numerically for different advanced fiber (Glass/Carbon/Kevlar) reinforcement in polymer matrix composite on the eigen-characteristics. Mehar et al. [21] examined the vibration frequencies of multi-walled carbon nanotube-reinforced polymer composite structure via a generic higher-order shear deformation kinematics for different panel geometries. Dewangan et al. [22] presented numerical eigenfrequency and experimental verification of variable cutout (square/rectangular) borne layered glass/epoxy flat/curved panel structure. Also, many studies reported the application of applied soft computing methods for the prediction of the behavior of the complex system [23-30].

A key issue in the various engineering field is that the prediction of the properties, behavior, and performance of different systems is an important aspect [31-42]. By considering the mentioned necessities and in the field of wave propagation in composite beams and plates, Ref [43] presented a comprehensive formulation on the wave dispersion of a high speed rotating two dimensional-functionally graded (2D-FG) nanobeam. They solved their complex formulation via an analytical method and reported that the rotating speed is the most effective parameter. By employing the new

version of couple stress theory, Global matrix, and Legendre orthogonal polynomial methods, Liu et al. [44] had a try for reporting the characteristics of the propagated wave in a functionally graded (FG) microplate. They reported that by controlling the couple stress parameter, we will have the grater phase velocity in the aspect of wave propagation. Gao et al. [45] reported a mathematical framework to analyze the propagated waves in the graphene nanoplatelets (GPLs) reinforced porous FG plate via a well-known mixture method. Ebrahimi et al. [46] were able to provide results on the characteristics of propagated waves in a compositionally nonlocal plate in which the structure was located in a high-temperature environment. Also, they considered the shear deformation in each element of the structure. Finally, they found that without doubt, the nonlocal effect has a bolded role on the characteristics of the phase velocity. Safaei et al. [47] tried to report characteristics of the propagated waves in a CNTs reinforced FG thermoelastic plate via the HSDT and Mori–Tanaka method. Their important achievement was that the thermal stress and adding a small amount of CNTs could make a remarkable effect on the wave velocity in the structure. Also, Mehar et al. [16, 48-51] examined the mechanical responses of CNT reinforced composites with the aid of HSDT. In addition, the stability of the complex structure is investigated in Refs [52, 53].

In the field of propagated wave characteristics in the shell, Karami et al. [54] developed a mathematical model for wave dispersion analysis in an imperfect higher-order nanoshell. They provided some evidence that the sensitivity of the prospected waves to the nonlocal effects, temperature, and humidity should be considered. Bakhtiari et al. [55] provided some results on the wave propagation of the FG shell in which fluid flow through the shell is considered. The dispersion behavior of the wave in the MHC reinforced shell is investigated by Ebrahimi et al. [56]. They used the Eshelby-Mori-Tanaka method and rule of mixture in order to predict the equivalent mechanical properties of nanocomposite shell. They found out the impact of nanosize reinforcements is more effective than the macro size reinforcements for improving the phase velocity of the compositionally shell. Abad et al. [57] published an article in which they presented a formulation about the wave propagation problem of a thick sandwich plate. They smarted the plate by patching a piezoelectric layer on the top face of the structure, and they considered Maxwell's assumptions in their computational approach. Habibi et al. [58] studied the phase velocity characteristics in a nanoshell reinforced with GPLs. When they compared their result with molecular simulation, observed that the size effect should be considered via nonlocal strain gradient theory (NSGT) as an exact size-dependent theory. As a practical outcome, they reported

that the thickness of the piezoelectric layer would have more effect on the characteristics of propagated waves in the nanoshell. Li et al. [59] succeeded in publishing an article in which they examined the wave propagation of a smart plate via a semi-analytical method. They modeled a GPLs reinforced plate, which is covered with a piezoelectric actuator. They used the Reissner-Mindlin plate theory and Hamilton's principle for developing the governing equations. The application of their result was that GPLs in a matrix can play a positive role in structural health monitoring and improve wave propagation in the structures, especially smart structures. Also, some researchers tried to predict the static and dynamic properties of different structures and materials via neural network solution [60-73].

Based on the extremely detailed exploration in the literature by the authors, no one can deny there is a study on the wave propagation of the MHC reinforced doubly curved panel in the viscoelastic medium. Therefore, in the current report, the characteristics of the propagated wave in the MHC reinforced doubly curved panel covered with the viscoelastic foundation is investigated. HSDT is utilized to express the displacement kinematics. Rule of the mixture and modified Halpin–Tsai model are engaged to provide the effective material constant of the MHC reinforced doubly curved panel. By employing Hamilton's principle, the governing equations of the structure are derived. The results demonstrate that the CNTs' weight fraction, various MHC patterns, radius to total thickness ratio, and carbon fibers angel have an important role in the phase velocity characteristics of the MHC reinforced doubly curved panel.

Mathematical modeling:

Figure 1 shows an MHC reinforced doubly curved panel in the viscoelastic medium. The thickness and the shell curvatures of the doubly curved panel are presented by h, R_x, and R_y, respectively.

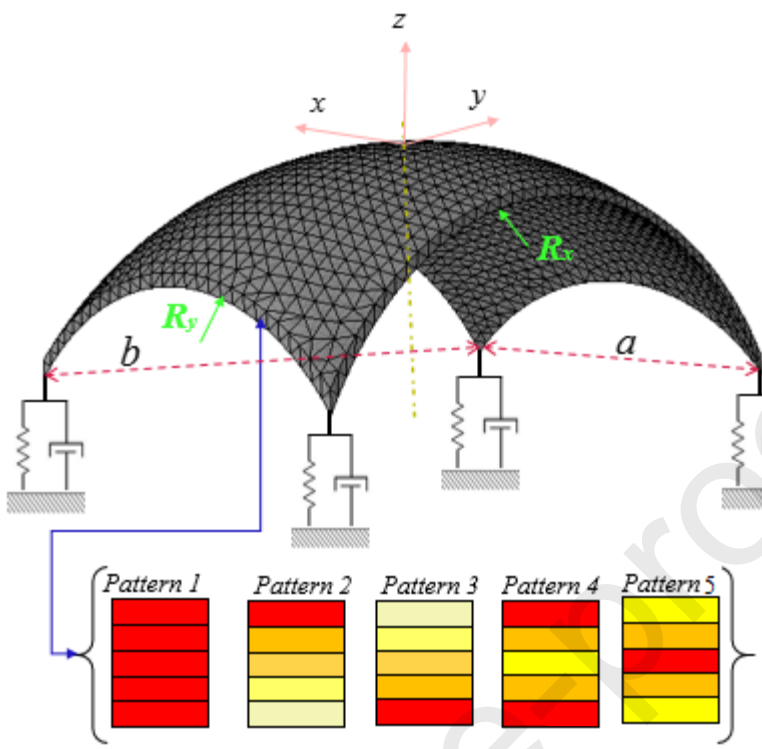

Figure1: A schematic of the MHC reinforced doubly curved panel in the viscoelastic medium

MHC Reinforcement:

The procedure of homogenization is made of two main steps based upon the Halpin-Tsai model together with a micromechanical theory. The first stage is engaged with computing the effective characteristics of the composite reinforced with carbon fiber as following [74]

$$E_{11} = V_F E_{11}^F + V_{NCM} E^{NCM} \tag{1}$$

$$\frac{1}{E_{22}} = 1/E_{22}^F + V_{NCM}/E^{NCM} - V_F V_{NCM} - \frac{(\nu^F)^2 E^{NCM}/E_{22}^F + (\nu^{NCM})^2 E_{22}^F/E^M - 2\nu^{NCM}\nu^F}{V_F E_{22}^F + V_{NCM} E^{NCM}} \tag{2}$$

$$\frac{1}{G_{12}} = \frac{V_{NCM}}{G^{NCM}} + \frac{V_F}{G_{12}^F} \tag{3}$$

$$\rho = V_F \rho^F + V_{NCM} \rho^{NCM} \tag{4}$$

$$\nu_{12} = V_F \nu^F + V_{NCM} \nu^{NCM} \tag{5}$$

Here, elasticity modulus, mass density, Poisson's ratio, and shear modulus are symbolled via ρ, E, G and ν. The superscripts of the matrix and fiber are *NCM* and *F*, respectively. Also, have:

$$V_F + V_{NCM} = 1 \tag{6}$$

The second step is organized to obtain the effective characteristics of the nanocomposite matrix reinforced with CNTs with the aid of the extended Halpin-Tsai micromechanics as follows [74]

$$E = \frac{5}{8}\left(\frac{1+2\beta_{dd}V_{CNT}}{1-\beta_{dd}V_{CNT}}\right)E^M + \frac{3}{8}\left(\frac{\beta_{dl}V_{CNT}(2l^{CNT}/d^{CNT})+1}{1-\beta_{dl}V_{CNT}}\right) \tag{7}$$

Here, β_{dd} and β_{dl} would be computed as the following expression

$$\begin{aligned} \beta_{dl} &= (E_{11}^{CNT}/E^M) - (d^{CNT}/4t^{CNT}) \big/ (E_{11}^{CNT}/E^M) + (l^{CNT}/2t^{CNT}) \\ \beta_{dd} &= (E_{11}^{CNT}/E^M) - (d^{CNT}/4t^{CNT}) \big/ (E_{11}^{CNT}/E^M) + (d^{CNT}/2t^{CNT}) \end{aligned} \tag{8}$$

Volume fraction, thickness, length, elasticity modulus, weight fraction, and diameter of CNTs are V_{CNT}, t^{CNT}, l^{CNT}, E^{CNT}, W_{CNT}, and d^{CNT}. Also, the volume fraction of the matrix and elasticity modulus of the matrix are V_M and E^M, respectively. So, The CNTs' volume fraction can be formulated as below [56]:

$$V_{CNT}^* = \frac{W_{CNT}}{W_{CNT} + \left(\frac{\rho^{CNT}}{\rho^M}\right)(1-W_{CNT})} \tag{9}$$

Also, the effective volume fraction of CNTs can be formulated as follows:

$$
\begin{aligned}
&V_{CNT} = V_{CNT}^{*} && \text{FG-UD} && (Pattern\,1)\\
&V_{CNT} = V_{CNT}^{*}\left(1+\frac{2\xi_j}{h}\right) && \text{FG-V} && (Pattern\,2)\\
&V_{CNT} = V_{CNT}^{*}\left(1-\frac{2\xi_j}{h}\right) && \text{FG-A} && (Pattern\,3)\\
&V_{CNT} = V_{CNT}^{*}\frac{\left|\xi_j\right|}{h} && \text{FG-X} && (Pattern\,4)\\
&V_{CNT} = V_{CNT}^{*}\left(1-2\frac{\left|\xi_j\right|}{h}\right) && \text{FG-O} && (Pattern\,5)
\end{aligned}
\tag{10}
$$

Where $\xi_j = \left(\frac{1}{2}+\frac{1}{2N_t}-\frac{j}{N_t}\right)h$ j=1,2,...,N_t.

Also, have

$$V_{CNT} + V_M = 1 \tag{11}$$

Also, Poisson's ratio, mass density, and shear modulus will be calculated as:

$$\rho = V_{CNT}\rho^{CNT} + V_M\rho^{M} \tag{12}$$

$$\nu = \nu^{M} \tag{13}$$

$$G = \frac{E}{2(1+\nu)} \tag{14}$$

Kinematic relations

Based on HSDT, the fields of doubly curved panel displacement can be given by [75, 76]:

$$
\begin{aligned}
u &= u_0 + zu_1 + z^2u_2 + z^3u_3\\
v &= v_0 + zv_1 + z^2v_2 + z^3v_3\\
w &= w_0
\end{aligned}
\tag{15}
$$

in which u_0, v_0, and w_0 show, respectively, the mid-plane displacements along the x, y, and z directions. Moreover, u_1 and v_1 are shear rotations while u_2, v_2, u_3, and v_3 are the higher-order terms. Furthermore, the non-zero shear and normal strains can be defined as follows [75, 76]:

$$\begin{Bmatrix} \varepsilon_{xx} \\ \varepsilon_{yy} \\ \gamma_{xy} \\ \gamma_{xz} \\ \gamma_{yz} \end{Bmatrix} = \begin{bmatrix} \frac{\partial u_0}{\partial x} + z\frac{\partial u_1}{\partial x} + z^2\frac{\partial u_2}{\partial x} + z^3\frac{\partial u_3}{\partial x} + \frac{w_0}{R_x} \\ \frac{\partial v_0}{\partial y} + z\frac{\partial v_1}{\partial y} + z^2\frac{\partial v_2}{\partial y} + z^3\frac{\partial v_3}{\partial y} + \frac{w_0}{R_y} \\ \frac{\partial u_0}{\partial y} + z\frac{\partial u_1}{\partial y} + z^2\frac{\partial u_2}{\partial y} + z^3\frac{\partial u_3}{\partial y} + \frac{\partial v_0}{\partial x} + z\frac{\partial v_1}{\partial x} + z^2\frac{\partial v_2}{\partial x} + z^3\frac{\partial v_3}{\partial x} \\ u_1 + 2zu_2 + 3z^2u_3 + \frac{\partial w_0}{\partial x} - \frac{1}{R_x}\left(u_0 + zu_1 + z^2u_2 + z^3u_3\right) \\ v_1 + 2zv_2 + 3z^2v_3 + \frac{\partial w_0}{\partial y} - \frac{1}{R_y}\left(v_0 + zv_1 + z^2v_2 + z^3v_3\right) \end{bmatrix} \tag{16}$$

Also, the strain-stress equations of the structure can be given as [9, 10, 77-81]:

$$\begin{bmatrix} \sigma_{xx} \\ \sigma_{yy} \\ \sigma_{xy} \\ \sigma_{xz} \\ \sigma_{yz} \end{bmatrix} = \begin{bmatrix} \hat{\bar{Q}}_{11} & \hat{\bar{Q}}_{12} & 0 & 0 & \hat{\bar{Q}}_{16} \\ \hat{\bar{Q}}_{21} & \hat{\bar{Q}}_{22} & 0 & 0 & \hat{\bar{Q}}_{26} \\ 0 & 0 & \hat{\bar{Q}}_{44} & \hat{\bar{Q}}_{45} & 0 \\ 0 & 0 & \hat{\bar{Q}}_{45} & \hat{\bar{Q}}_{55} & 0 \\ \hat{\bar{Q}}_{16} & \hat{\bar{Q}}_{26} & 0 & 0 & \hat{\bar{Q}}_{66} \end{bmatrix} \begin{bmatrix} \varepsilon_{xx} \\ \varepsilon_{yy} \\ \varepsilon_{xy} \\ \varepsilon_{xz} \\ \varepsilon_{yz} \end{bmatrix} \tag{17}$$

Where[82]

$$\hat{\bar{Q}}_{11} = \cos^4\theta\tilde{Q}_{11} + 2\sin^2\theta\cos^2\theta\left(\tilde{Q}_{12} + 2\tilde{Q}_{66}\right) + \sin^4\theta\tilde{Q}_{22} \tag{18a}$$

$$\hat{\bar{Q}}_{12} = \sin^2\theta\cos^2\theta\left(\tilde{Q}_{11} + \tilde{Q}_{22} - 4\tilde{Q}_{66}\right) + \left(\sin^4\theta + \cos^4\theta\right)\tilde{Q}_{12} \tag{18b}$$

$$\hat{\bar{Q}}_{16} = \cos^3\theta\sin\theta\left(2\tilde{Q}_{11} - 2\tilde{Q}_{12} - \tilde{Q}_{66}\right) + \cos\theta\sin^3\theta\left(\tilde{Q}_{66} + 2\tilde{Q}_{12} - 2\tilde{Q}_{22}\right) \tag{18c}$$

$$\hat{\bar{Q}}_{22} = \sin^4\theta\tilde{Q}_{11} + 2\sin^2\theta\cos^2\theta\tilde{Q}_{12} + \cos^4\theta\tilde{Q}_{22} + 2\sin^2\theta\cos^2\theta\left(\tilde{Q}_{12} + 2\tilde{Q}_{66}\right) \tag{18d}$$

$$\hat{\bar{Q}}_{26} = \cos^3\theta\sin\theta\left(2\tilde{Q}_{12} - 2\tilde{Q}_{22} + \tilde{Q}_{66}\right) + \cos\theta\sin^3\theta\left(2\tilde{Q}_{11} - 2\tilde{Q}_{12} - \tilde{Q}_{66}\right) \tag{18e}$$

$$\hat{\bar{Q}}_{44} = \cos^2\theta\tilde{Q}_{44} + \sin^2\theta\tilde{Q}_{55} \tag{18f}$$

$$\hat{\bar{Q}}_{45} = \cos\theta\sin\theta\left(\tilde{Q}_{55} - \tilde{Q}_{44}\right) \tag{18g}$$

$$\hat{\tilde{Q}}_{55} = \cos^2\theta \tilde{Q}_{55} + \sin^2\theta \tilde{Q}_{44} \tag{18h}$$

$$\hat{\tilde{Q}}_{66} = \tilde{Q}_{66}\left(\cos^2\theta - \sin^2\theta\right)^2 + 4\sin^2\theta\cos^2\theta\left(\tilde{Q}_{11} + \tilde{Q}_{22} - 2\tilde{Q}_{12}\right) \tag{18i}$$

The terms used in Eq. (18) would be obtained as

$$\tilde{Q}_{11} = \frac{E_{11}}{1-\nu_{12}\nu_{21}},\ \tilde{Q}_{12} = \frac{\nu_{12}E_{22}}{1-\nu_{12}\nu_{21}},\ \tilde{Q}_{22} = \frac{E_{22}}{1-\nu_{12}\nu_{21}},\ \tilde{Q}_{44} = G_{12},\ \tilde{Q}_{55} = G_{23},\ \tilde{Q}_{66} = G_{13}.$$

2.4. Extended Hamilton's principle:

To obtain the governing equations, the extended Hamilton's principle can be formulated as follows [9, 10, 77-81, 83]:

$$\int_{t_1}^{t_2} (\delta U - \delta K + \delta W)dt = 0 \tag{19}$$

The strain energy components can be given as follows:

$$\delta U = \frac{1}{2}\iiint_V \sigma_{ij}\delta\varepsilon_{ij}dV =$$

$$= \iint_A \left[\begin{array}{l} N_{xx}\left(\frac{\partial\delta u_0}{\partial x} + \frac{\delta w_0}{R_x}\right) + M_{xx}\frac{\partial\delta u_1}{\partial x} + Q_{xx}\frac{\partial\delta u_2}{\partial x} + P_{xx}\frac{\partial\delta u_3}{\partial x} \\ +N_{yy}\left(\frac{\partial\delta v_0}{\partial y} + \frac{\delta w_0}{R_y}\right) + M_{yy}\frac{\partial\delta v_1}{\partial y} + Q_{yy}\frac{\partial\delta v_2}{\partial y} + P_{yy}\frac{\partial\delta v_3}{\partial y} \\ +N_{yz}(\delta v_1 + \frac{\partial\delta w_0}{\partial y} - \frac{\delta v_0}{R_y}) + M_{yz}(2\delta v_2 - \frac{\delta v_1}{R_y}) + Q_{yz}(3\delta v_3 - \frac{\delta v_2}{R_y}) - \frac{P_{yz}}{R_y}(\delta v_3) \\ +N_{xz}(\delta u_1 + \frac{\partial\delta w_0}{\partial x} - \frac{\delta u_0}{R_x}) + M_{xz}(2\delta u_2 - \frac{\delta u_1}{R_x}) + Q_{xz}(3\delta u_3 - \frac{\delta u_2}{R_x}) - \frac{P_{xz}}{R_x}(\delta u_3) \\ +N_{xy}\left(\frac{\partial\delta u_0}{\partial y} + \frac{\partial\delta v_0}{\partial x}\right) + M_{xy}\left(\frac{\partial\delta u_1}{\partial y} + \frac{\partial\delta v_1}{\partial x}\right) + P_{xy}\left(\frac{\partial\delta u_2}{\partial y} + \frac{\partial\delta v_2}{\partial x}\right) + Q_{xy}\left(\frac{\partial\delta u_3}{\partial y} + \frac{\partial\delta v_3}{\partial x}\right) \end{array}\right] dA \tag{20-a}$$

which:

$$\left\{N_{ij}, M_{ij}, Q_{ij}, P_{ij}\right\} = \int_z \left\{\sigma_{ij}, z\sigma_{ij}, z^2\sigma_{ij}, z^3\sigma_{ij}\right\}dz \tag{20-b}$$

Also, the kinetic energy of the structure can be defined as bellow:

$$\delta K = \int_Z \iint_A \rho \left\{ (\frac{\partial u}{\partial t}\frac{\partial \delta u}{\partial t}) + \frac{\partial v}{\partial t}\frac{\partial \delta v}{\partial t} + \frac{\partial w}{\partial t}\frac{\partial \delta w}{\partial t} \right\} dA \tag{21}$$

The first variation of the applied work due to viscoelastic foundation can be presented as below:

$$\delta W = \iint_A (K_w w \delta w + C_d \dot{w} \delta w)\, dA \tag{22}$$

In the above equation, K_w, and C_d are the elastic and viscose parameter of the foundation. Consequently, by substituting Eqs. (22), (21), and (20-a) in Eq. (19), motion equations of the MHC reinforced doubly curved panel can be achieved. It should be noted that the motion and governing equations of the structure are given in "Appendix."

Solution procedure:

The fields of displacement for wave dispersion analysis of the structure can be expressed as follows [84]:

$$\begin{Bmatrix} u_0 \\ v_0 \\ w_0 \\ u_1 \\ v_1 \\ u_2 \\ v_2 \\ u_3 \\ v_3 \end{Bmatrix} = \begin{Bmatrix} U_0 \exp(sx + n\theta - \omega t)i \\ V_0 \exp(sx + n\theta - \omega t)i \\ W_0 \exp(sx + n\theta - \omega t)i \\ U_1 \exp(sx + n\theta - \omega t)i \\ V_1 \exp(sx + n\theta - \omega t)i \\ U_2 \exp(sx + n\theta - \omega t)i \\ V_2 \exp(sx + n\theta - \omega t)i \\ U_3 \exp(sx + n\theta - \omega t)i \\ V_3 \exp(sx + n\theta - \omega t)i \end{Bmatrix} \tag{23}$$

where s and n are wave number along with the directions of x and y, respectively, also ω is called frequency. With replacing Eq. (23) into governing equations achieve to:

$$([K]+\omega[C]-\omega^2[M])\{d\}=\{0\} \tag{24}$$

where

$$\{d\}=\{u_0 \quad v_0 \quad w_0 \quad u_1 \quad v_1 \quad u_2 \quad v_2 \quad u_3 \quad v_3\} \tag{25}$$

Also, the phase velocity can be calculated by Eq. (26):

$$c=\frac{\omega}{s} \tag{26}$$

Validation:

The obtained results for the perfect panel are compared with the results of Refs. [85, 86]. These results are listed in Table 1. From this table, it can be observed that the current results are validated with the published research. Note that the dimensionless form of the frequency is as below:

$$\Omega=\omega\frac{a^2}{h}\sqrt{\frac{\rho_M}{E_M}} \tag{27}$$

Table 1: Comparison of the first dimensionless natural frequency of simply-supported CNT reinforced composite square perfect panel (a/h = 10).

V_{CNT}	Ref [85]	Ref [86]	Present study
11%	0.1319	0.1357	0.1350
14%	0.1400	0.1438	0.1429
17%	0.1638	0.1685	0.1658

For more verification, the fundamental frequencies of the laminated moderately thick plates resting on elastic foundations are calculated by the eigenvalue problem. In Table 2, non-dimensional fundamental frequencies of the symmetrically laminated cross-ply plate (0°,90°,90°,0°) are shown as compared to different E_1/E_2.

Table 2: Non-dimensional fundamental frequency of simply-supported cross-ply laminated square plate with G_{12}/E_2=0.6, G_{13}/E_2=0.6, G_{23}/E_2=0.5, a=b=1, υ=0.25

E_1/E_2	Ref [87]	Ref [88]	Presented study	Discrepancy
10	8.2982	8.2981	8.5485	3%
20	9.5671	9.5671	10.0328	4%
30	10.326	10.326	10.6318	2%
40	10.824	10.854	11.0045	1%

Results:

In this part, a comprehensive investigation is carried out to demonstrate the effects of various parameters on the phase velocity response of an MHC reinforced doubly curved panel in the viscoelastic foundation. The geometrical and material characteristics of constituent materials would be presented in Table 3.

Table 3: Material properties of the MHC reinforcement [89]

Carbon fiber	E_{11}^{F} [Gpa]	E_{22}^{F} [Gpa]	G_{12}^{F} [Gpa]	ρ^{F} [kg/m^3]	ν^{F}	α_{11}^{F} [×10^{-6}/k]	α_{22}^{F} [×10^{-6}/k]		
	233.05	23.1	8.96	1750	0.2	-0.54	10.08		
Epoxy Matrix	E^{m} [Gpa]	ν^{m}		ρ^{m} [kg/m^3]		α^{m} [×10^{-6}/k]			
	3.51	0.34		1200		45			
Carbon nanotube	E_{11}^{F} [Tpa]	$E_{22}^{CNT} = E_{33}^{CNT}$ [Tpa]	$G_{12}^{CNT} = G_{13}^{CNT}$ [Tpa]	ν_{12}^{CNT}	ρ^{CNT} [kg/m^3]	α^{CNT} [×10^{-6}/k]	l^{CNT} [μm]	d^{CNT} [nm]	t^{CNT} [nm]
	5.6466	7.0800	1.9445	0.175	1350	3.4584	25	1.4	0.34

In Figure 2 the phase velocity of the hybrid nanocomposite doubly curved panel versus wave number is presented with attention to the effect of the damping parameter C_d of the viscoelastic foundation.

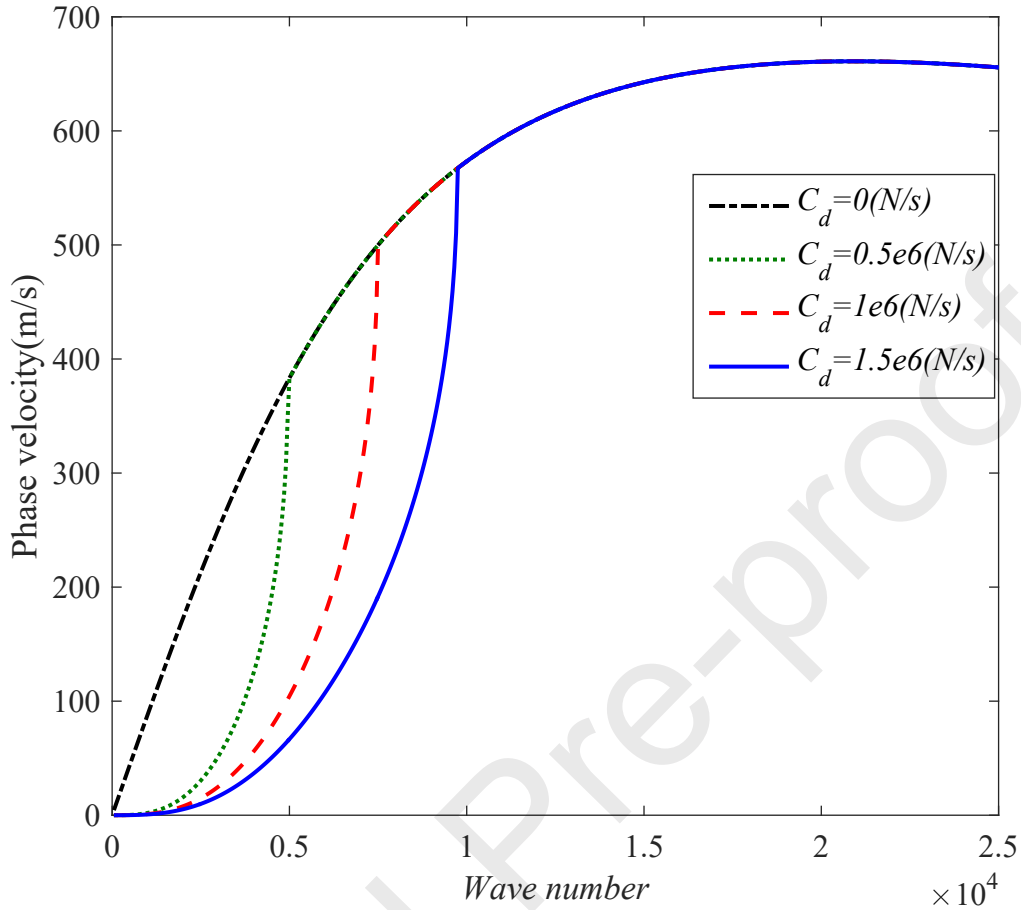

Figure 2: The effect of the damping parameter of the viscoelastic foundation on the characteristic of the propagated wave in the MHC reinforced panel

The general result which could be seen from the given diagrams in Figure 2 is that when the foundation is used, as the wave number increases, the phase velocity improves. With more precision in Figure 2 can see that if the damping parameter of the viscoelastic foundation is equal to zero, as the wave number increases, the phase velocity increases logarithmic while for $C_d > 0$, the relation between wavenumber and phase velocity changes from exponential increase to logarithmic boost. The most impressive result is that, as the phase velocity of the panel increases, the damping parameter loses its effectiveness. Also, at the initial value of the wavenumber, we could find a positive effect from C_d on the wave response of the structure, but this impact will be ineffective at the higher wavenumber. As we mentioned, there is a range for the wavenumber in which there are not any effects from the damping parameter of the foundation on the phase velocity

and this range can be stretched by each amplification in the damping parameter of the viscoelastic foundation. In Figure 3 the phase velocity of the hybrid nanocomposite doubly curved panel versus wave number is presented with attention to the effect of elastic parameter of the viscoelastic foundation.

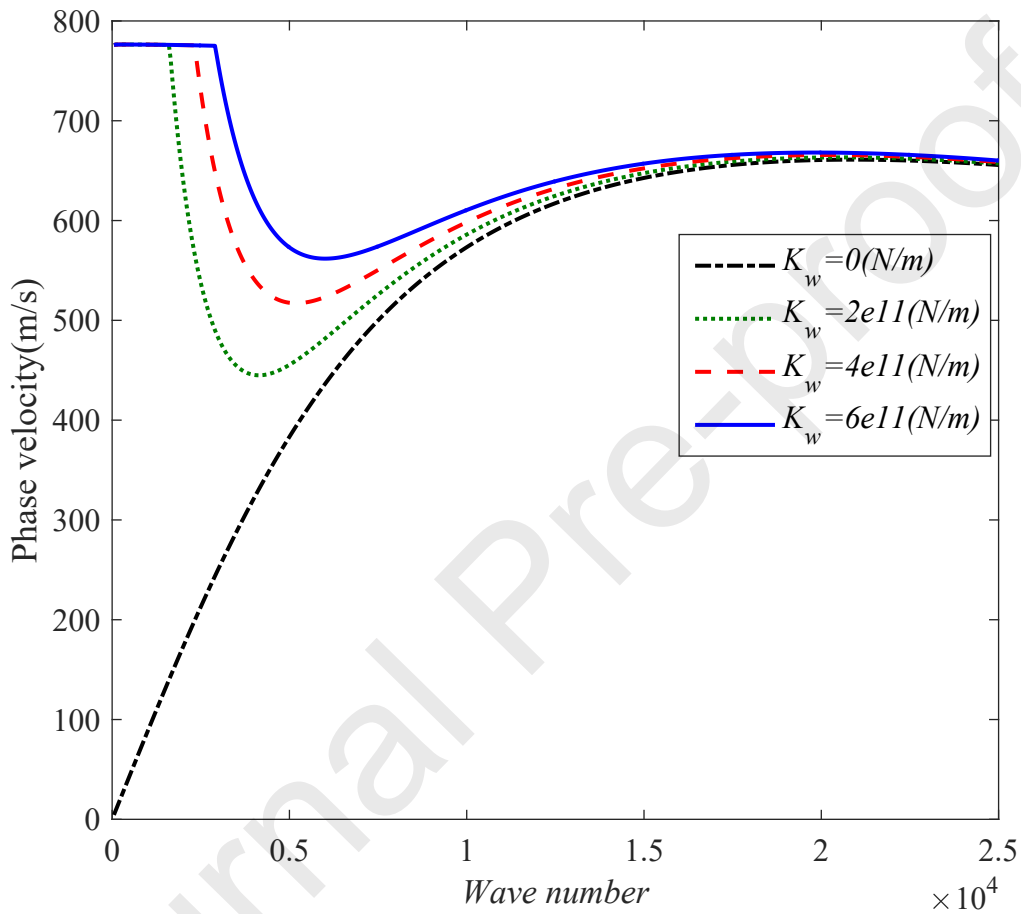

Figure 3: The effect of the elastic parameter of the foundation on the characteristic of the propagated wave in the MHC reinforced panel

Based on Figure 3 can conclude that when the elastic parameter of the foundation is equal to zero, as wave number increases, the phase velocity improves, while this relation will be complex by considering $K_w > 0$. For each K_w, at first, the phase velocity of the panel is constant by increasing the wavenumber, and at the medium values of the wavenumber, the phase velocity will be falling, so after a minimum value, the relation changes to increase. Another important result from Figure

4 is that the impact of K_w on the wave response of the structure is considerable for $0.4 < K_w e4 < 1.5$, and this effect is negligible at the initial and high value of the wavenumber.

In Figure 4 the phase velocity of the hybrid nanocomposite doubly curved panel versus K_w is presented with attention to the different values of the wavenumber.

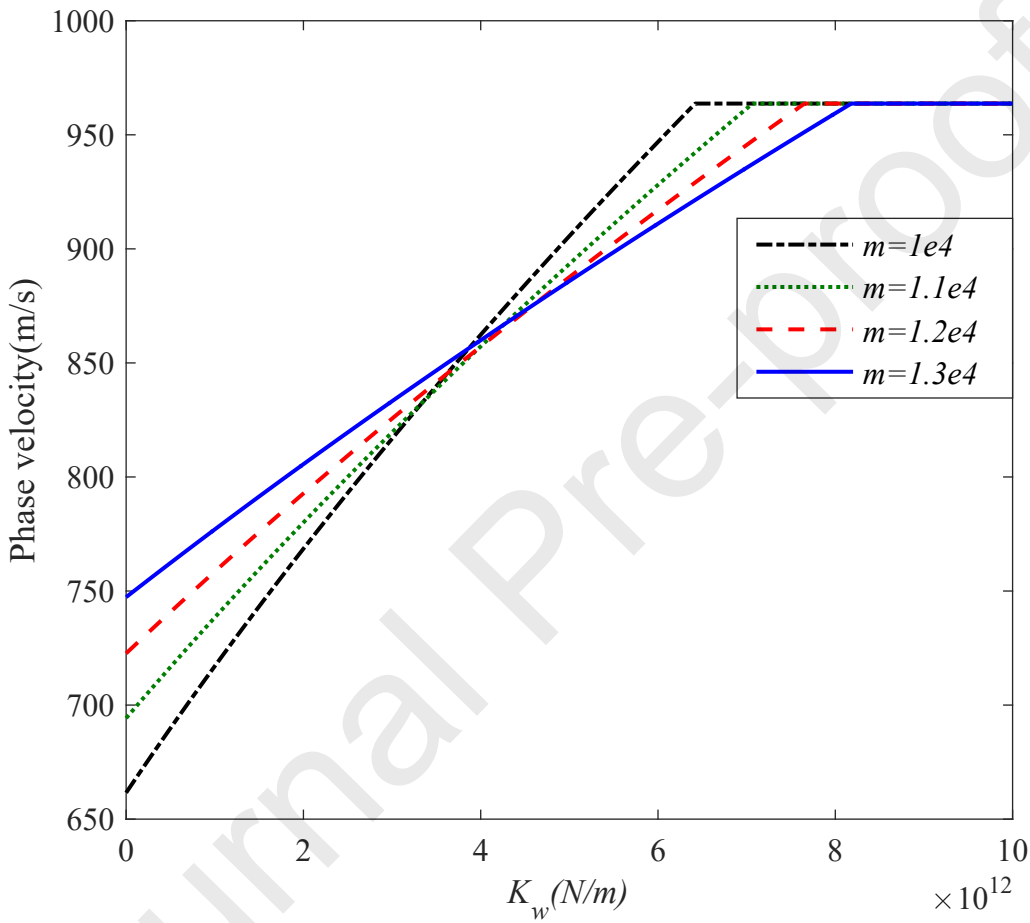

Figure 4: The effects of wavenumber and elastic parameter of the foundation on the characteristic of the propagated wave in the MHC reinforced panel

One of the bolded result in Figure 4 is that there are three ranges for K_w that in those regions, the relation between wavenumber and phase velocity is direct, indirect, and ineffective. Also, for each wavenumber, boosting the $K_w$can be an encouragement for improving the phase velocity of the panel, linearly and this impact from $K_w$on the wave propagation of the structure will change to be ineffective at the higher value of K_w. Also, this ineffective range of K_w on the phase, velocity can

be limited due to having each rise in the wavenumber. As a practical conclusion from Figure 4, K_w =4e12 is a critical value for the elastic factor of the viscoelastic foundation that the relation between wavenumber and phase velocity will change from direct to indirect.

In Figure 5 the phase velocity of the hybrid nanocomposite doubly curved panel versus C_d is presented with attention to the different values of the wavenumber.

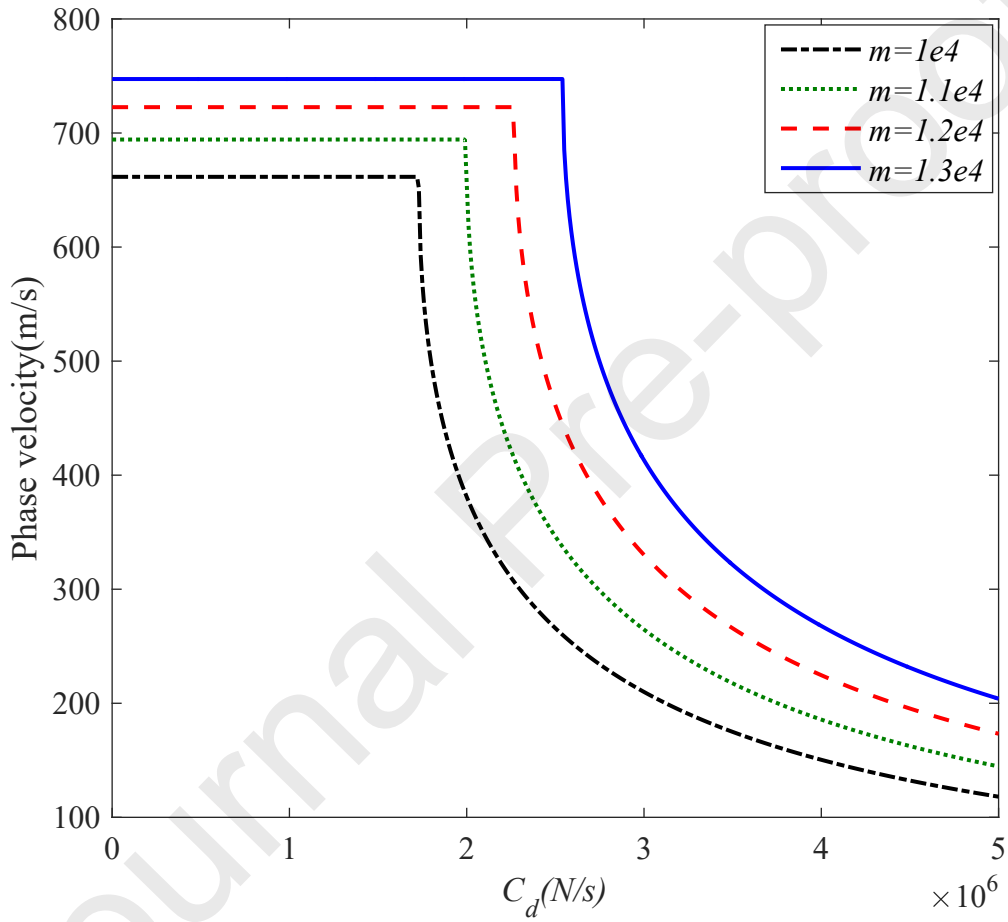

Figure 5: The effects of wavenumber and damping parameter of the foundation on the characteristic of the propagated wave in the MHC reinforced panel

If we have excellent attention to Figure 5 could be seen that for each value of the wavenumber, due to each increase in C_d, in the beginning, no change in phase velocity of the panel is observed due to changing the damping parameter and after a certain amount of C_d, the phase velocity decreases exponentially with having an increase in the damping parameter. Also, the phase

velocity in the panel will decrease after a specific value of the C_d and this value is decreased due to an increase in the wavenumber.

The wave information of an MHC reinforced doubly curved panel is investigated in Figure 6. In this section, we try to discuss the effects of wavenumber and different FG patterns on the phase velocity of the structure.

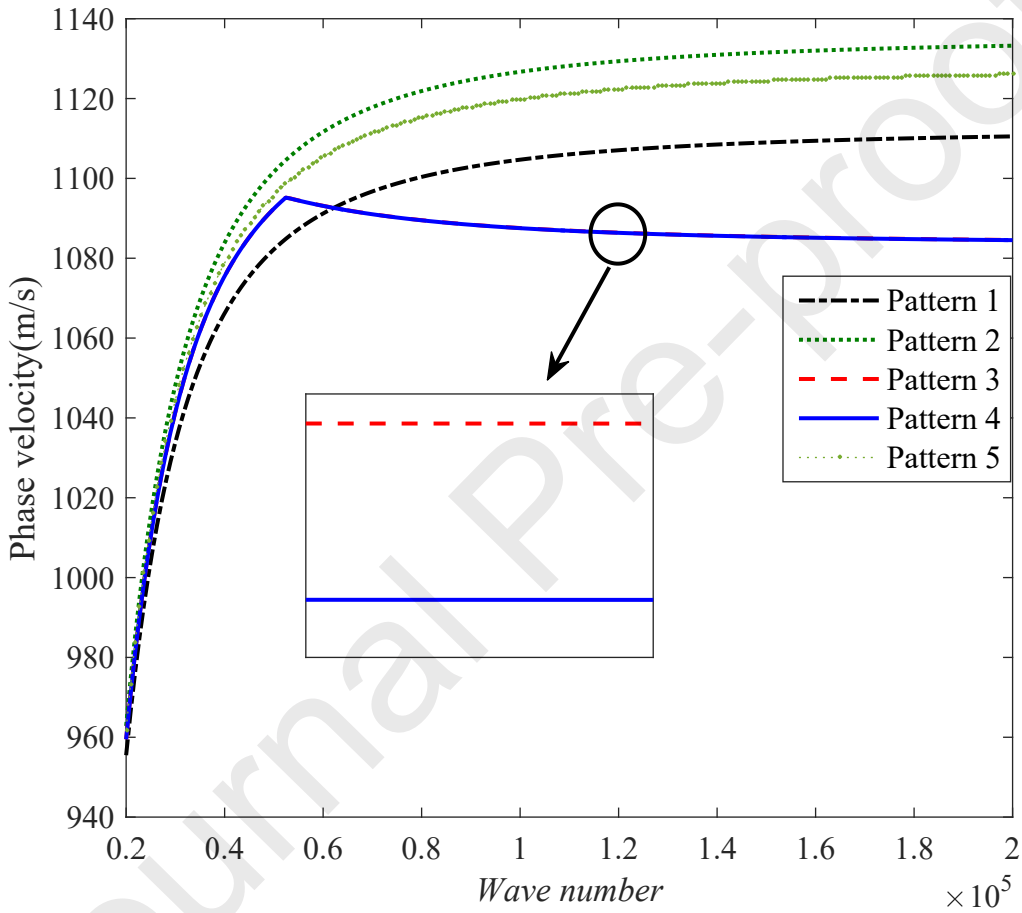

Figure 6: The effects of wavenumber and different FG patterns on the characteristic of the propagated wave in the MHC reinforced panel

The bolded result in Figure 6 is that for patterns 1, 2, and 5, increasing the wave number can be an encouragement for improving the phase velocity of the composite panel. Also, for patterns 3 and 4, the relation between wavenumber and phase velocity will change from logarithmic increase to exponential decrease, and for each wavenumber, the impact of patterns 3 and 4 on the phase

velocity of the panel is not considerable, or these patterns have the same phase velocity responses. As a practical result, For $m \leq$ 0.5e5, when the structure is made by Patterns 1 and 2 we can see the lowest and highest phase velocity in the panel while For $m >$ 0.5e5, the lowest and highest phase velocity are for the panel, which is made by Patterns 4 and 2, respectively.

Reported data in Figure 7 is shown to have a deep presentation about the effects of the carbon fibers angel (θ/π) and CNTs' weight fraction (W_{CNT}) on the wave responses of the sandwich structure.

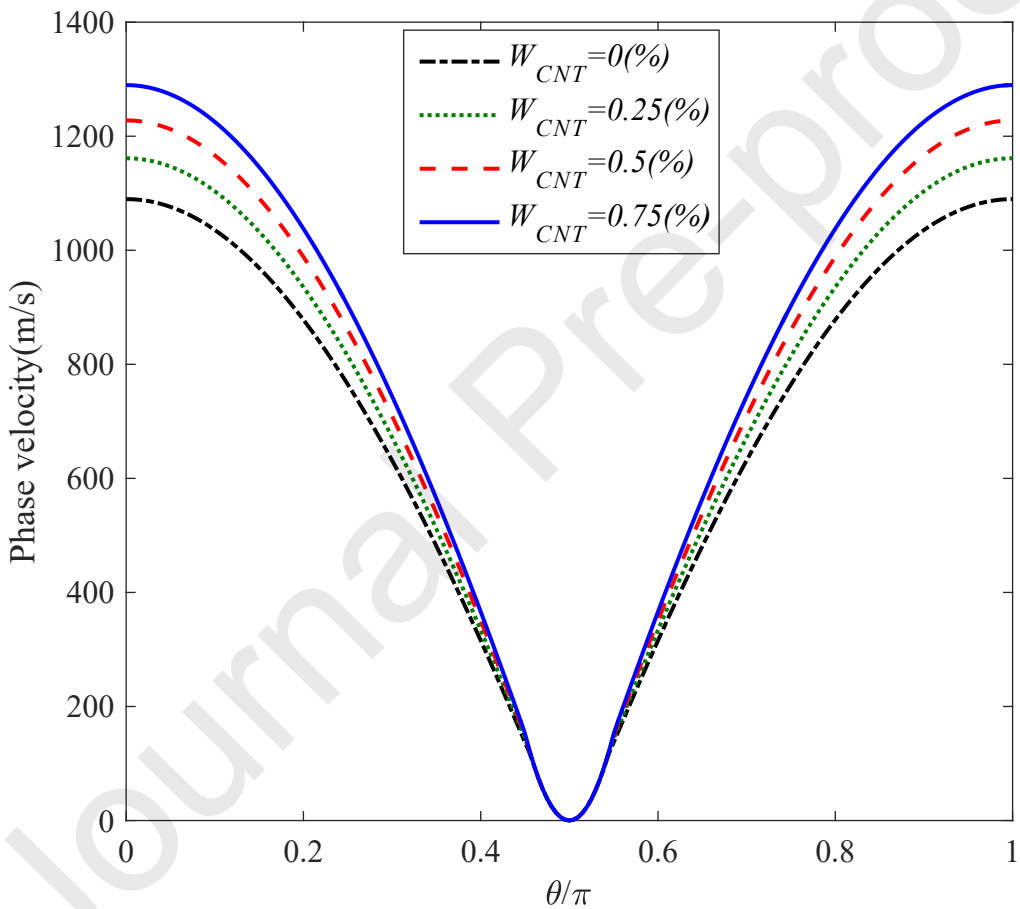

Figure 7: The phase velocity versus carbon fibers angel for various CNTs weight fraction

The most general result in Figure 7 is that for each value of W_{CNT}, when the fibers angel is less than $\pi/2$, the phase velocity decreases and this trend will be revers for the fibers angel more than $\pi/2$. As another explanation, if the fibers distribute in the matrix vertically, changing the weight

fraction of CNTs cannot play any role on the wave response of the panel and as the fibers become horizontal, the effect of the W_{CNT} on the phase velocity becomes more dramatic.

The wave information of an MHC reinforced doubly curved panel is analysis in Figure 8 and in this section, we try to consider the influences of the C_d and θ/π on the phase velocity of the compositionally structure, simultaneously.

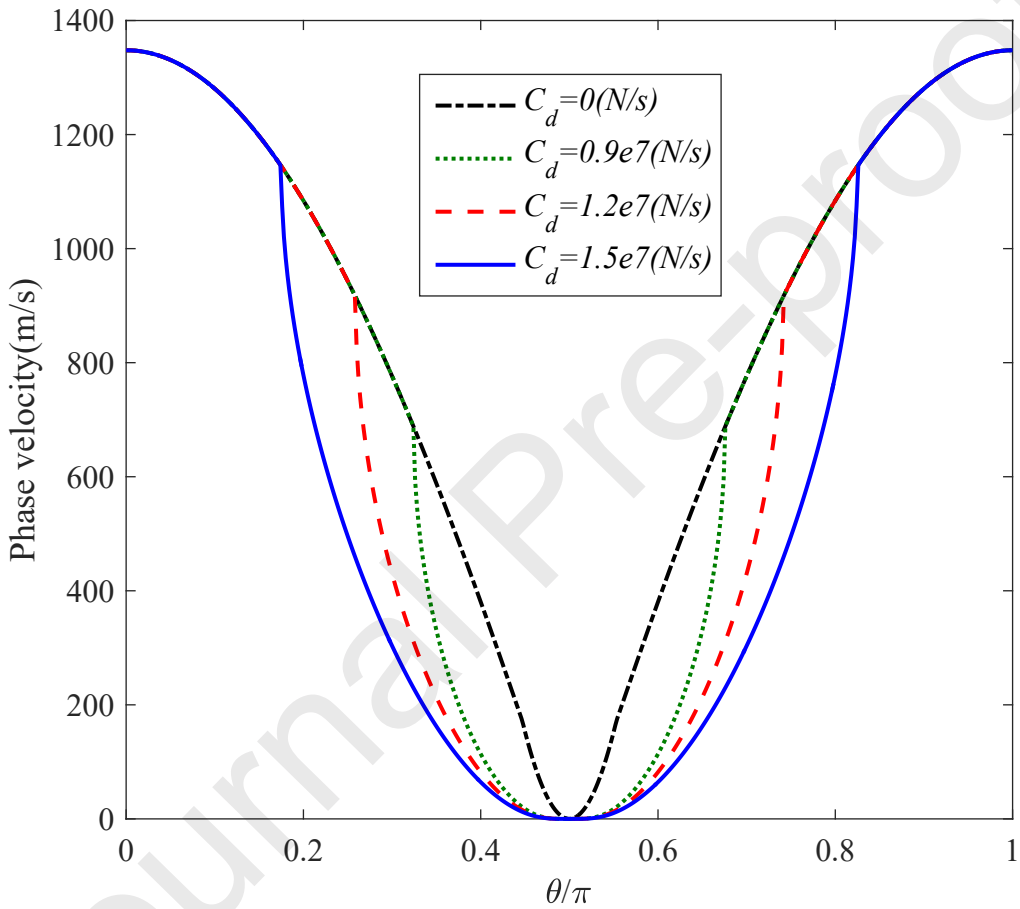

Figure 8: The phase velocity versus carbon fibers angel for various C_d

Based on Figure 8 can conclude that when the orientation of the carbon fibers in the matrix is being close to the vertical axis the effect of C_d on the phase velocity of the panel will be evident and C_d has a positive impact on the wave propagation response of the panel. As shown in Figure 7, $\theta/\pi =$ 0.5 is the critical fibers angel, and this critical value will be a range of angel by increasing the damping factor of the foundation. As an applicable report from Figure 8, for $0 \leq \theta/\pi \leq 0.2$ and 0

$\leq \theta/\pi \leq 0.2$, there is no effect from C_d on phase velocity. Besides, in the specific range of θ/π, the damping factor of the foundation has an ineffective role on the phase velocity of the panel and the range will become small by boosting the C_d.

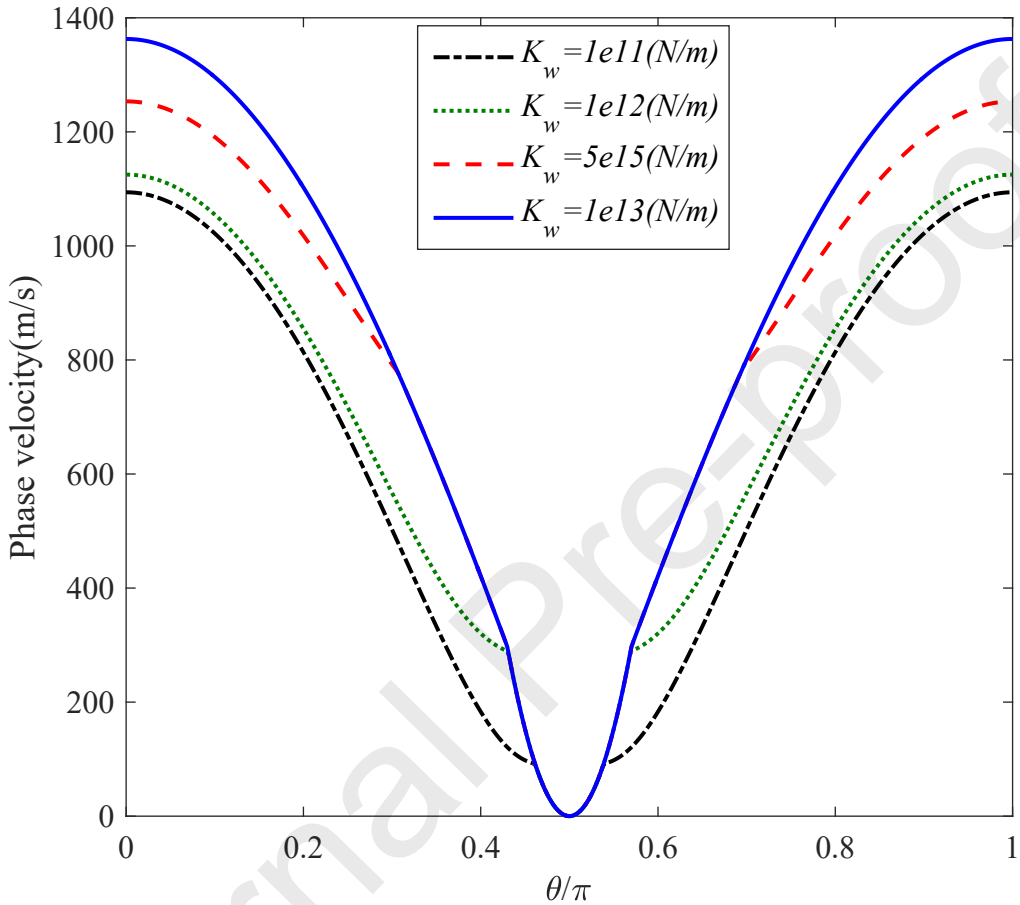

Figure 9: The phase velocity versus carbon fibers angel for various K_w

According to Figure 9 can conclude that when the orientation of the carbon fibers in the matrix is being close to the horizontal axis the effect of K_w on the phase velocity of the panel will be evident, and this impact is a positive point on the wave propagation response of the panel. As shown in Figure 8, $\theta/\pi = 0.5$ is the critical fibers angel, and in this range of fiber angle, there is not any effect from K_w on the phase velocity. As an applicable report from Figure 8, in a specific range of θ/π, the elastic factor of the foundation has an ineffective role on the phase velocity of the panel, and the range will be grate by boosting the K_w.

The provided results in Figures 10 and 11 encounter us with a study on the effects of V_f, R_x/h, and fibers angle (θ/π) on the wave propagation of the MHC reinforced doubly curved panel.

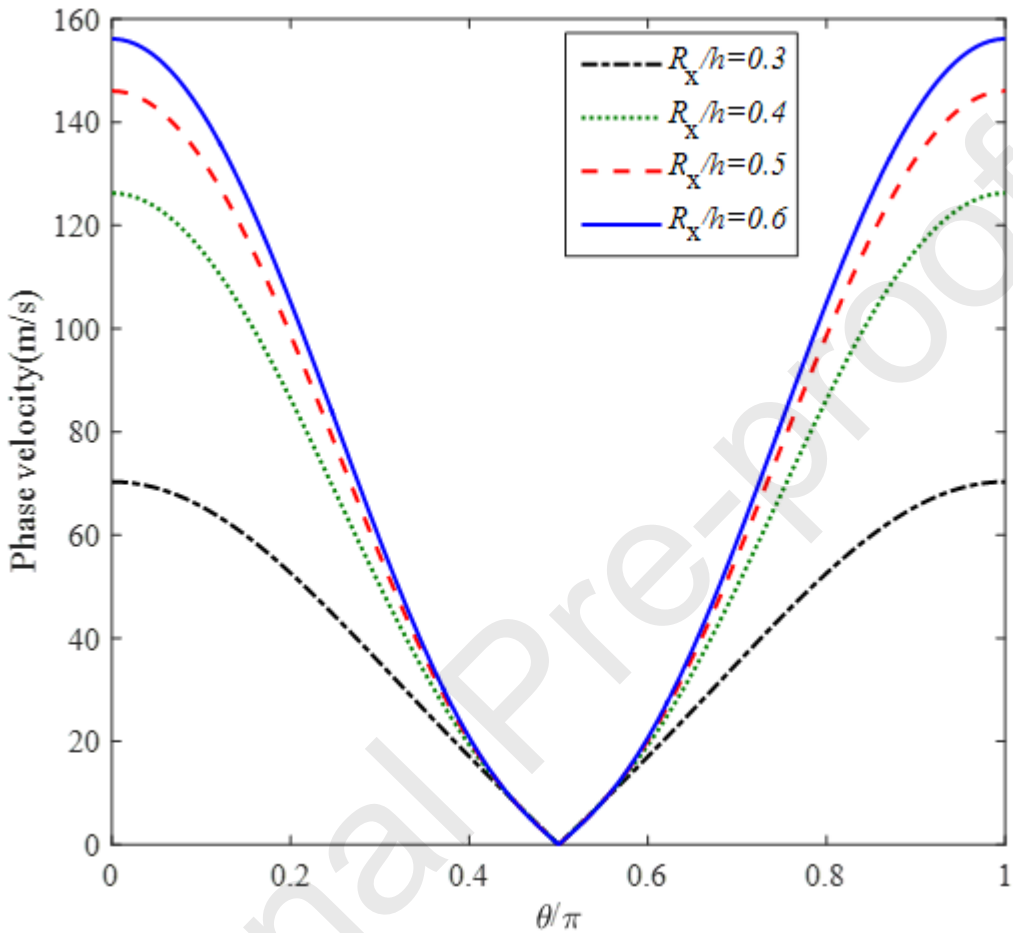

Figure 10: The phase velocity versus carbon fibers angel for various R_x/h

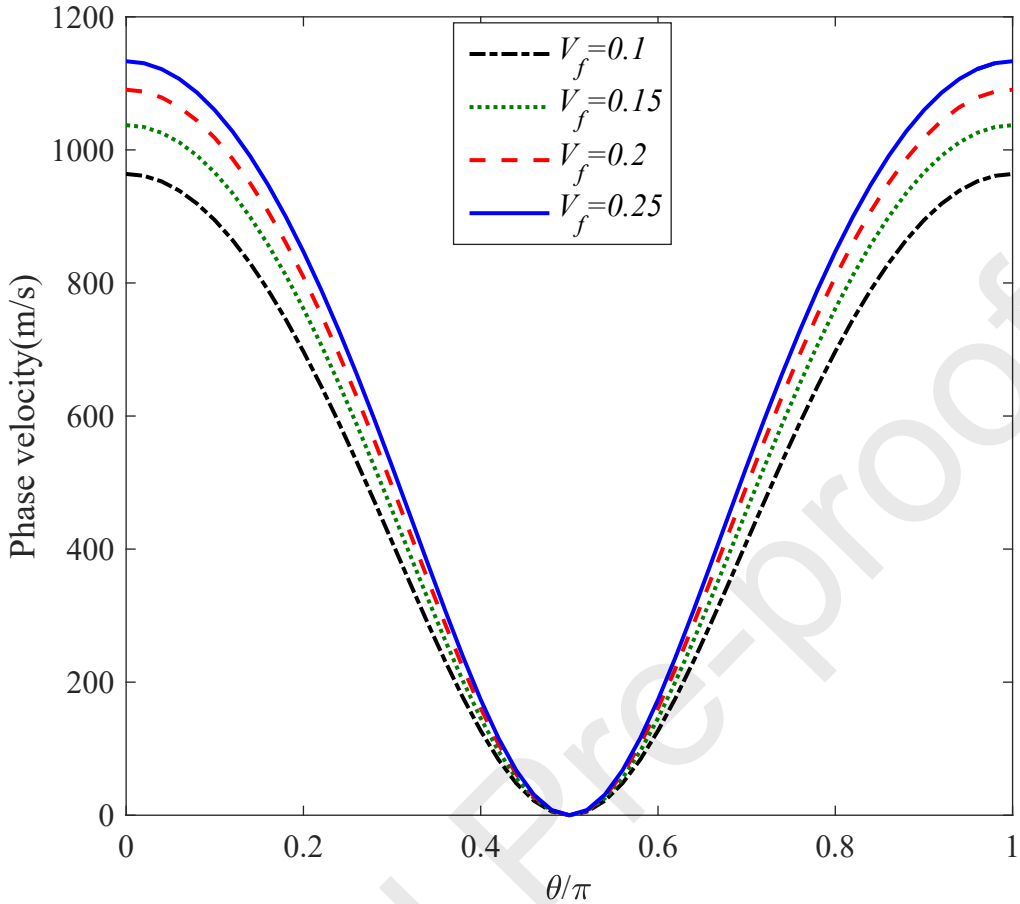

Figure 11: The phase velocity versus carbon fibers angel for various V_f.

With close attention to the provided diagrams in Figures 10 and 11 can see that as well as an improvement on the phase velocity of the structure due to increasing the volume fraction of the carbon fibers and R_x/h, the mentioned impact is more remarkable when the carbon fibers in the matrix are distributed horizontally. In addition, the more vertical carbon fibers will be a reason to decrease the impact of R_x/h of the structure on the phase velocity of the panel. For more detail, if the fibers are vertical, there is not any change in the phase velocity due to any change in the R_x/h. The main point of figures 10 and 11 is that the wave response of the MHC reinforced panel is more dependent on the carbon fibers angle, and the phase velocity will be zero if the fibers angle is 90°.

A comprehensive and comparative study is presented in Figure 12 for providing a conclusion about the impacts of wavenumber, carbon fibers angel, and C_d on the wave responses of the panel.

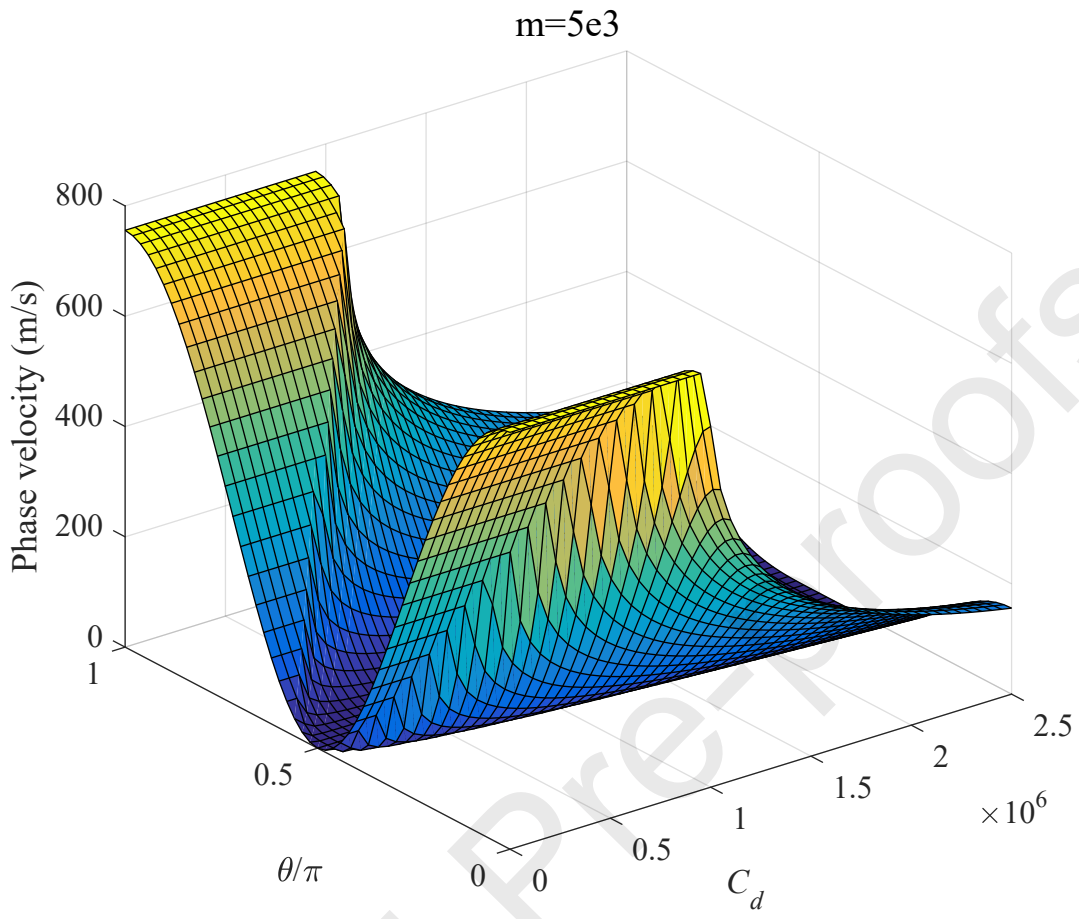

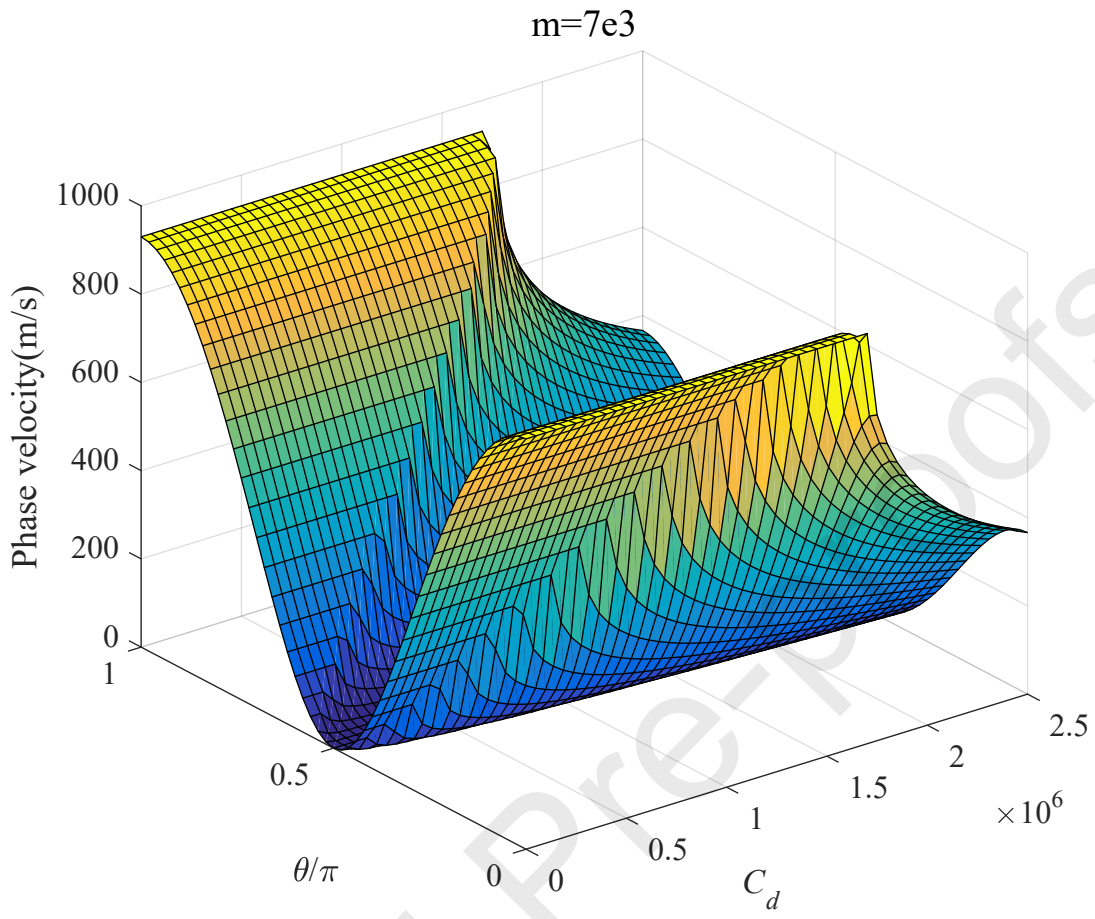

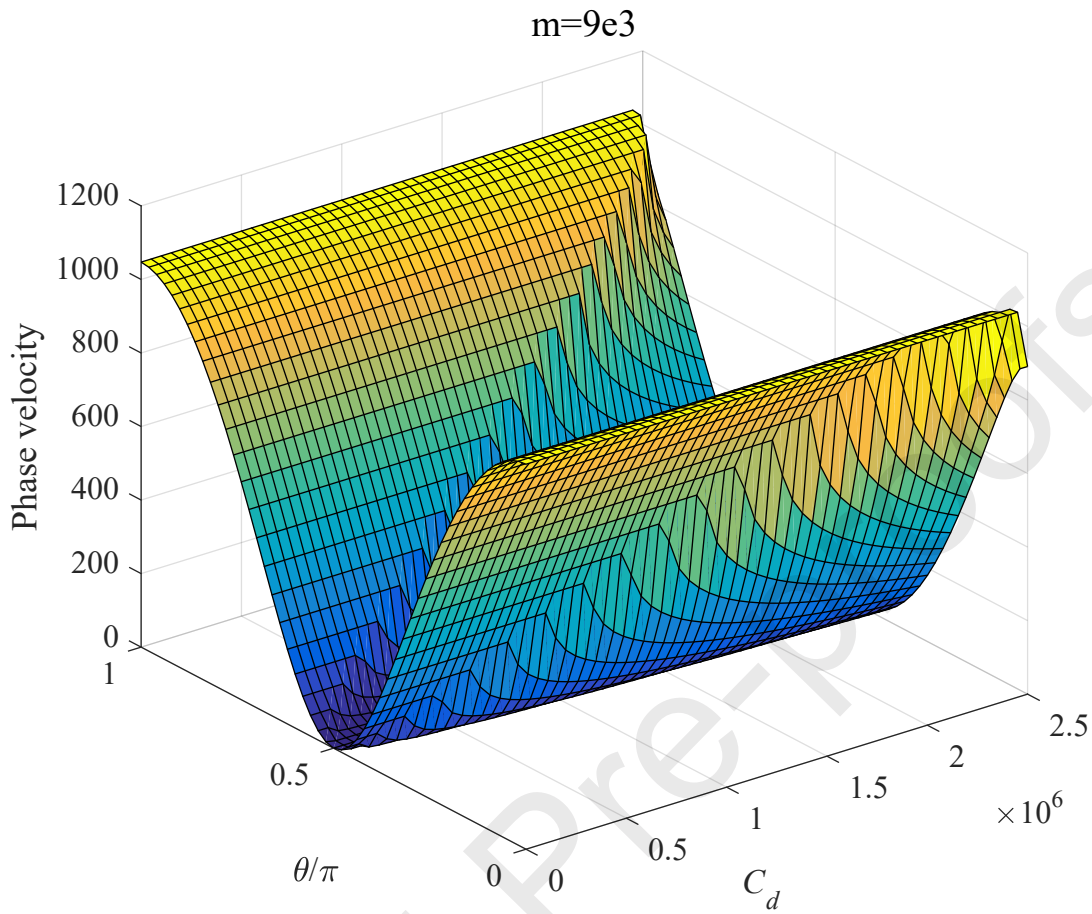

Figure 12: The impacts of wavenumber, the damping factor of the foundation, and fibers angle on the wave response of the panel

The principal result in Figure 12 is that as the wave number increases, the changes in phase velocity become much more dramatic by increasing the fibers' angel and damping factor of the foundation. In other words, the effects of θ/π and C_d on the phase velocity of the panel is highly dependent on the wavenumber. Also, the effect of fibers angle on phase velocity is intensified by increasing the wavenumber.

Diagrams in Figure 13 are shown to have a comparative study about the effects of K_w and fibers angel on the wave responses of the doubly carved panel.

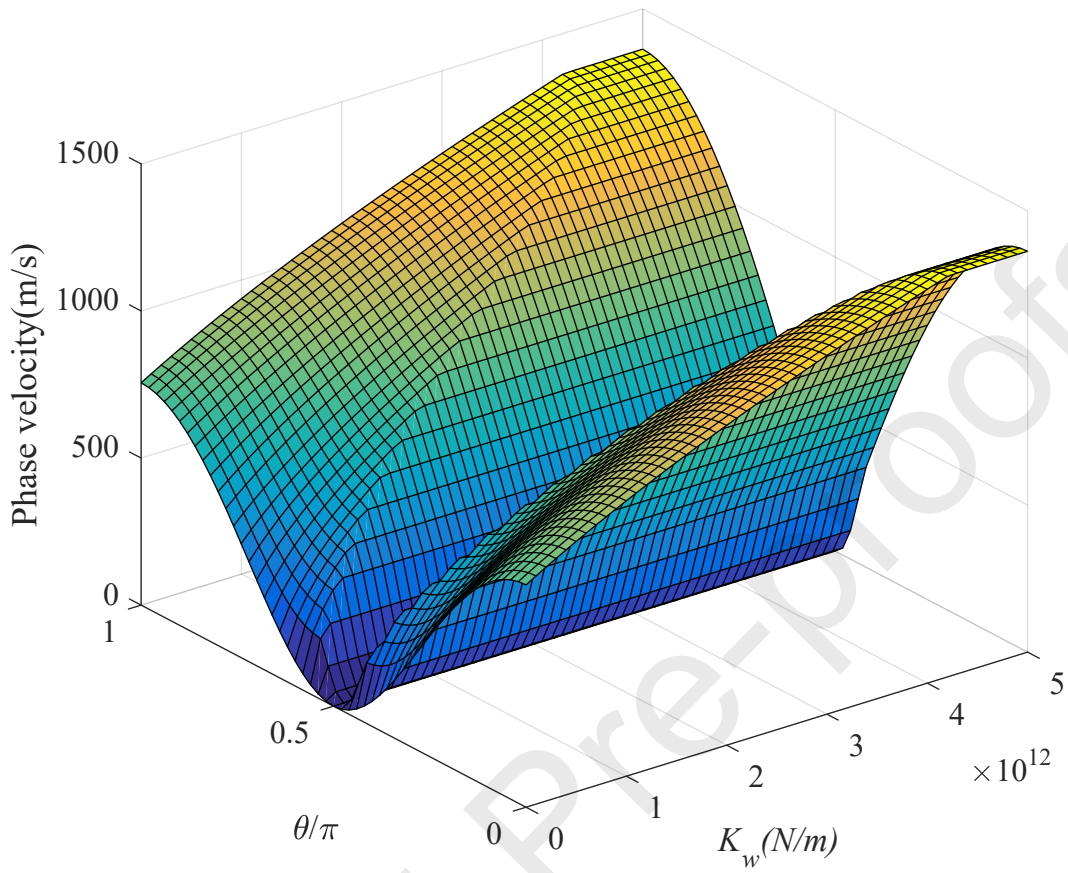

Figure 13: The impacts of K_w and fibers angle on the wave response of the panel

The principal result in Figure 13 is that as the K_w increases, the changes in phase velocity become much more dramatic by increasing the fibers' angel. In other words, the effects of θ/π on the phase velocity of the panel is highly dependent on the K_w. In addition, the effect of K_w on the phase, velocity is intensified when the fibers angel is more vertical.

Conclusion:

This article accomplished wave propagation analysis of the MHC reinforced doubly curved panel embedded in the viscoelastic foundation within the framework of HSDT. Rule of the mixture and modified Halpin–Tsai model was engaged to provide the effective material constant of the multi-hybrid nanocomposite panel. By employing Hamilton's principle, the governing equations of the structure were derived. Finally, the most bolded results of this paper were as follows:

- for $C_d > 0$, the relation between wavenumber and phase velocity changes from exponential increase to logarithmic boost and at the initial value of the wavenumber we could find a positive effect from C_d on the wave response of the structure, but this impact will be ineffective at the higher wavenumber.
- there is a critical value for the viscoelastic foundation in which the relation between wavenumber and phase velocity will change from direct to indirect.
- For $0 \leq \theta/\pi \leq 0.2$ and $0 \leq \theta/\pi \leq 0.2$, there is no any effects from C_d on phase velocity and in a specific range of θ/π, the damping factor of the foundation has an ineffective role in the phase velocity of the panel.
- the effects of θ/π and C_d on the phase velocity of the panel is hardly dependent on the wavenumber. Also, the effect of fiber angle on phase velocity intensifies by increasing the wavenumber.
- the effects of θ/π on the phase velocity of the panel is hardly dependent on the K_w and the effect of K_w on the phase, velocity intensifies when the fibers angel is more vertical.

Appendix:

The motion equations of the MHC reinforced doubly curved panel embedded in the viscoelastic foundation are given as follows:

$$
\begin{aligned}
&\delta u_0 : \frac{\partial N_{xx}}{\partial x} + \frac{\partial N_{xy}}{\partial y} + \frac{N_{xz}}{R_x} = I_0 \frac{\partial^2 u_0}{\partial t^2} + I_1 \frac{\partial^2 u_1}{\partial t^2} + I_2 \frac{\partial^2 u_2}{\partial t^2} + I_3 \frac{\partial^2 u_3}{\partial t^2}, \\
&\delta v_0 : \frac{\partial N_{yy}}{\partial y} + \frac{\partial N_{xy}}{\partial x} + \frac{N_{yz}}{R_y} = I_0 \frac{\partial^2 v_0}{\partial t^2} + I_1 \frac{\partial^2 v_1}{\partial t^2} + I_2 \frac{\partial^2 v_2}{\partial t^2} + I_3 \frac{\partial^2 v_3}{\partial t^2}, \\
&\delta w_0 : \frac{\partial N_{yz}}{\partial y} + \frac{\partial N_{xz}}{\partial x} - \frac{N_{xx}}{R_x} - \frac{N_{yy}}{R_y} - K_w w_0 + C \frac{\partial w_0}{\partial t} = I_0 \frac{\partial^2 w_0}{\partial t^2}, \\
&\delta u_1 : \frac{\partial M_{xx}}{\partial x} + \frac{\partial M_{xy}}{\partial y} + \frac{M_{xz}}{R_x} - N_{xz} = I_1 \frac{\partial^2 u_0}{\partial t^2} + I_2 \frac{\partial^2 u_1}{\partial t^2} + I_3 \frac{\partial^2 u_2}{\partial t^2} + I_4 \frac{\partial^2 u_3}{\partial t^2}, \\
&\delta v_1 : \frac{\partial M_{yy}}{\partial y} + \frac{\partial M_{xy}}{\partial x} + \frac{M_{yz}}{R_y} - N_{yz} = I_1 \frac{\partial^2 v_0}{\partial t^2} + I_2 \frac{\partial^2 v_1}{\partial t^2} + I_3 \frac{\partial^2 v_2}{\partial t^2} + I_4 \frac{\partial^2 v_3}{\partial t^2}, \\
&\delta u_2 : \frac{\partial Q_{xx}}{\partial x} + \frac{\partial Q_{xy}}{\partial y} + \frac{Q_{xz}}{R_x} - 2M_{xz} = I_2 \frac{\partial^2 u_0}{\partial t^2} + I_3 \frac{\partial^2 u_1}{\partial t^2} + I_4 \frac{\partial^2 u_2}{\partial t^2} + I_5 \frac{\partial^2 u_3}{\partial t^2}, \\
&\delta v_2 : \frac{\partial Q_{yy}}{\partial y} + \frac{\partial Q_{xy}}{\partial x} + \frac{Q_{yz}}{R_y} - 2M_{yz} = I_2 \frac{\partial^2 v_0}{\partial t^2} + I_3 \frac{\partial^2 v_1}{\partial t^2} + I_4 \frac{\partial^2 v_2}{\partial t^2} + I_5 \frac{\partial^2 v_3}{\partial t^2}, \\
&\delta u_3 : \frac{\partial P_{xx}}{\partial x} + \frac{\partial P_{xy}}{\partial y} + \frac{P_{xz}}{R_x} - 3Q_{xz} = I_3 \frac{\partial^2 u_0}{\partial t^2} + I_4 \frac{\partial^2 u_1}{\partial t^2} + I_5 \frac{\partial^2 u_2}{\partial t^2} + I_6 \frac{\partial^2 u_3}{\partial t^2}, \\
&\delta v_3 : \frac{\partial P_{yy}}{\partial y} + \frac{\partial P_{xy}}{\partial x} + \frac{P_{yz}}{R_y} - 3Q_{yz} = I_3 \frac{\partial^2 v_0}{\partial t^2} + I_4 \frac{\partial^2 v_1}{\partial t^2} + I_5 \frac{\partial^2 v_2}{\partial t^2} + I_6 \frac{\partial^2 v_3}{\partial t^2}.
\end{aligned}
\tag{1-a}
$$

Where

$$
\{I_i\} = \int_{-\frac{h}{2}}^{\frac{h}{2}} \rho \{z^i\} dz, \; i = 0:6 \tag{2-a}
$$

Finally, by substituting Eq. (20-b), and (2-a) in Eq. (1-a) the governing equations of the structure can be achieved.

Funding:

- National Natural Science Foundation of China (51675148).
- The Outstanding Young Teachers Fund of Hangzhou Dianzi University (GK160203201002/003).
- National Natural Science Foundation of China (51805475).
- This research was supported by the 2020 scientific promotion funded by Jeju National University.

References:

[1] V. Farhangi and M. Karakouzian, "Effect of fiber reinforced polymer tubes filled with recycled materials and concrete on structural capacity of pile foundations," *Applied Sciences,* vol. 10, p. 1554, 2020.

[2] M. H. Ghayesh, "Nonlinear vibration analysis of axially functionally graded shear-deformable tapered beams," *Applied Mathematical Modelling,* vol. 59, pp. 583-596, 2018.

[3] M. H. Ghayesh, "Viscoelastic mechanics of Timoshenko functionally graded imperfect microbeams," *Composite Structures,* vol. 225, p. 110974, 2019.

[4] M. H. Ghayesh, "Subharmonic dynamics of an axially accelerating beam," *Archive of Applied Mechanics,* vol. 82, pp. 1169-1181, 2012.

[5] M. H. Ghayesh, H. Farokhi, and G. Alici, "Subcritical parametric dynamics of microbeams," *International Journal of Engineering Science,* vol. 95, pp. 36-48, 2015.

[6] M. H. Ghayesh, "Nonlinear oscillations of FG cantilevers," *Applied Acoustics,* vol. 145, pp. 393-398, 2019.

[7] S. Chen, G. Wang, S. Zuo, and C. Yang, "Experimental Investigation on Microstructure and Permeability of Thermally Treated Beishan Granite," *Journal of Testing and Evaluation,* vol. 49, 2019.

[8] M. Oyarhossein, V. Khiali, K. Hosseinmostofi, M. Adineh, and H. Bayatghiasi, "Numerical Study of the Gap at the Base of the Bridge on the River Flow Parameters," 2019.

[9] A. Ghabussi, M. Habibi, O. NoormohammadiArani, A. Shavalipour, H. Moayedi, and H. Safarpour, "Frequency characteristics of a viscoelastic graphene nanoplatelet–reinforced composite circular microplate," *Journal of Vibration and Control,* p. 1077546320923930, 2020.

[10] M. Safarpour, A. Ghabussi, F. Ebrahimi, M. Habibi, and H. Safarpour, "Frequency characteristics of FG-GPLRC viscoelastic thick annular plate with the aid of GDQM," *Thin-Walled Structures,* vol. 150, p. 106683, 2020.

[11] E. Cheshmeh, M. Karbon, A. Eyvazian, D. Jung, T. Tran, M. Habibi*, et al.*, "Buckling and vibration analysis of FG-CNTRC plate subjected to thermo-mechanical load based on higher-order shear deformation theory," *Mechanics Based Design of Structures and Machines*.

[12] A. Shariati, H. Mohammad-Sedighi, K. K. Żur, M. Habibi, and M. Safa, "Stability and Dynamics of Viscoelastic Moving Rayleigh Beams with an Asymmetrical Distribution of Material Parameters," *Symmetry,* vol. 12, p. 586, 2020.

[13] M. A. Oyarhossein, A. a. Alizadeh, M. Habibi, M. Makkiabadi, M. Daman, H. Safarpour*, et al.*, "Dynamic response of the nonlocal strain-stress gradient in laminated polymer composites microtubes," *Scientific Reports,* vol. 10, p. 5616, 2020/03/27 2020.

[14] M. Habibi, A. Taghdir, and H. Safarpour, "Stability analysis of an electrically cylindrical nanoshell reinforced with graphene nanoplatelets," *Composites Part B: Engineering,* vol. 175, p. 107125, 2019.

[15] K. Mehar, P. Mishra, and S. Panda, "Numerical investigation of thermal frequency responses of graded hybrid smart nanocomposite (CNT-SMA-Epoxy) structure," *Mechanics of Advanced Materials and Structures,* pp. 1-13, 2020.

[16] K. Mehar, S. K. Panda, and N. Sharma, "Numerical investigation and experimental verification of thermal frequency of carbon nanotube-reinforced sandwich structure," *Engineering Structures,* vol. 211, p. 110444, 2020.

[17] H. K. Pandey, C. K. Hirwani, N. Sharma, P. V. Katariya, H. C. Dewangan, and S. K. Panda, "Effect of nano glass cenosphere filler on hybrid composite eigenfrequency responses-An FEM approach and experimental verification," *Advances in nano research,* vol. 7, pp. 419-429, 2019.

[18] P. V. Katariya, K. Mehar, and S. K. Panda, "Nonlinear dynamic responses of layered skew sandwich composite structure and experimental validation," *International Journal of Non-Linear Mechanics,* p. 103527, 2020.

[19] K. Mehar, S. K. Panda, A. Dehengia, and V. R. Kar, "Vibration analysis of functionally graded carbon nanotube reinforced composite plate in thermal environment," *Journal of Sandwich Structures & Materials,* vol. 18, pp. 151-173, 2016.

[20] P. Sahu, N. Sharma, and S. K. Panda, "Numerical prediction and experimental validation of free vibration responses of hybrid composite (Glass/Carbon/Kevlar) curved panel structure," *Composite Structures,* vol. 241, p. 112073, 2020.

[21] K. Mehar, S. K. Panda, and T. R. Mahapatra, "Theoretical and experimental investigation of vibration characteristic of carbon nanotube reinforced polymer composite structure," *International Journal of Mechanical Sciences,* vol. 133, pp. 319-329, 2017.

[22] H. C. Dewangan, N. Sharma, C. K. Hirwani, and S. K. Panda, "Numerical eigenfrequency and experimental verification of variable cutout (square/rectangular) borne layered glass/epoxy flat/curved panel structure," *Mechanics Based Design of Structures and Machines,* pp. 1-18, 2020.

[23] X. Zhao, D. Li, B. Yang, C. Ma, Y. Zhu, and H. Chen, "Feature selection based on improved ant colony optimization for online detection of foreign fiber in cotton," *Applied Soft Computing,* vol. 24, pp. 585-596, 2014.

[24] M. Wang and H. Chen, "Chaotic multi-swarm whale optimizer boosted support vector machine for medical diagnosis," *Applied Soft Computing,* vol. 88, p. 105946, 2020.

[25] X. Zhao, X. Zhang, Z. Cai, X. Tian, X. Wang, Y. Huang*, et al.*, "Chaos enhanced grey wolf optimization wrapped ELM for diagnosis of paraquat-poisoned patients," *Computational biology and chemistry,* vol. 78, pp. 481-490, 2019.

[26] X. Xu and H.-L. Chen, "Adaptive computational chemotaxis based on field in bacterial foraging optimization," *Soft Computing,* vol. 18, pp. 797-807, 2014.

[27] L. Shen, H. Chen, Z. Yu, W. Kang, B. Zhang, H. Li*, et al.*, "Evolving support vector machines using fruit fly optimization for medical data classification," *Knowledge-Based Systems,* vol. 96, pp. 61-75, 2016.

[28] M. Wang, H. Chen, B. Yang, X. Zhao, L. Hu, Z. Cai*, et al.*, "Toward an optimal kernel extreme learning machine using a chaotic moth-flame optimization strategy with applications in medical diagnoses," *Neurocomputing,* vol. 267, pp. 69-84, 2017.

[29] Y. Xu, H. Chen, J. Luo, Q. Zhang, S. Jiao, and X. Zhang, "Enhanced Moth-flame optimizer with mutation strategy for global optimization," *Information Sciences,* vol. 492, pp. 181-203, 2019.

[30] H. Chen, Q. Zhang, J. Luo, Y. Xu, and X. Zhang, "An enhanced Bacterial Foraging Optimization and its application for training kernel extreme learning machine," *Applied Soft Computing,* vol. 86, p. 105884, 2020.

[31] N.-S. Gao, X.-Y. Guo, B.-Z. Cheng, Y.-N. Zhang, Z.-Y. Wei, and H. Hou, "Elastic wave modulation in hollow metamaterial beam with acoustic black hole," *IEEE Access,* vol. 7, pp. 124141-124146, 2019.

[32] N. Gao, Z. Wei, R. Zhang, and H. Hou, "Low-frequency elastic wave attenuation in a composite acoustic black hole beam," *Applied Acoustics,* vol. 154, pp. 68-76, 2019.

[33] N. Gao and Y. Zhang, "A low frequency underwater metastructure composed by helix metal and viscoelastic damping rubber," *Journal of Vibration and Control,* vol. 25, pp. 538-548, 2019.

[34] N. Gao, H. Hou, and J. H. Wu, "A composite and deformable honeycomb acoustic metamaterial," *International Journal of Modern Physics B,* vol. 32, p. 1850204, 2018.

[35] N. Gao, J. H. Wu, L. Yu, and H. Hou, "Ultralow frequency acoustic bandgap and vibration energy recovery in tetragonal folding beam phononic crystal," *International Journal of Modern Physics B,* vol. 30, p. 1650111, 2016.

[36] X. Tian, Z. Song, and J. Wang, "Study on the propagation law of tunnel blasting vibration in stratum and blasting vibration reduction technology," *Soil Dynamics and Earthquake Engineering,* vol. 126, p. 105813, 2019.

[37] B. Mou, Y. Bai, and V. Patel, "Post-local buckling failure of slender and over-design circular CFT columns with high-strength materials," *Engineering Structures,* vol. 210, p. 110197, 2020.

[38] C. Guo, M. Hu, Z. Li, F. Duan, L. He, Z. Zhang*, et al.*, "Structural hybridization of bimetallic zeolitic imidazolate framework (ZIF) nanosheets and carbon nanofibers for efficiently sensing α-synuclein oligomers," *Sensors and Actuators B: Chemical,* vol. 309, p. 127821, 2020.

[39] B. Mou, X. Li, Q. Qiao, B. He, and M. Wu, "Seismic behaviour of the corner joints of a frame under biaxial cyclic loading," *Engineering Structures,* vol. 196, p. 109316, 2019.

[40] B. Mou, F. Zhao, Q. Qiao, L. Wang, H. Li, B. He*, et al.*, "Flexural behavior of beam to column joints with or without an overlying concrete slab," *Engineering Structures,* vol. 199, p. 109616, 2019.

[41] X. Luo, J. Guo, P. Chang, H. Qian, F. Pei, W. Wang*, et al.*, "ZSM-5@ MCM-41 composite porous materials with a core-shell structure: Adjustment of mesoporous orientation basing on interfacial electrostatic interactions and their application in selective aromatics transport," *Separation and Purification Technology,* vol. 239, p. 116516, 2020.

[42] H. Chen, G. Zhang, D. Fan, L. Fang, and L. Huang, "Nonlinear Lamb Wave Analysis for Microdefect Identification in Mechanical Structural Health Assessment," *Measurement,* p. 108026, 2020.

[43] S. Faroughi, A. Rahmani, and M. Friswell, "On wave propagation in two-dimensional functionally graded porous rotating nano-beams using a general nonlocal higher-order beam model," *Applied Mathematical Modelling,* vol. 80, pp. 169-190, 2020.

[44] C. Liu, J. Yu, W. Xu, X. Zhang, and B. Zhang, "Theoretical study of elastic wave propagation through a functionally graded micro-structured plate base on the modified couple-stress theory," *Meccanica,* pp. 1-15, 2020.

[45] W. Gao, Z. Qin, and F. Chu, "Wave propagation in functionally graded porous plates reinforced with graphene platelets," *Aerospace Science and Technology,* p. 105860, 2020.

[46] F. Ebrahimi, M. R. Barati, and A. Dabbagh, "A nonlocal strain gradient theory for wave propagation analysis in temperature-dependent inhomogeneous nanoplates," *International Journal of Engineering Science,* vol. 107, pp. 169-182, 2016.

[47] B. Safaei, R. Moradi-Dastjerdi, Z. Qin, K. Behdinan, and F. Chu, "Determination of thermoelastic stress wave propagation in nanocomposite sandwich plates reinforced by clusters of carbon nanotubes," *Journal of Sandwich Structures & Materials,* p. 1099636219848282, 2019.

[48] K. Mehar and S. K. Panda, "Nonlinear deformation and stress responses of a graded carbon nanotube sandwich plate structure under thermoelastic loading," *Acta Mechanica,* vol. 231, pp. 1105-1123, 2020.

[49] K. Mehar and S. K. Panda, "Multiscale modeling approach for thermal buckling analysis of nanocomposite curved structure," *Advances in Nano Research,* vol. 7, p. 181, 2019.

[50] K. Mehar and S. K. Panda, "Theoretical deflection analysis of multi-walled carbon nanotube reinforced sandwich panel and experimental verification," *Composites Part B: Engineering,* vol. 167, pp. 317-328, 2019.

[51] K. Mehar, S. K. Panda, Y. Devarajan, and G. Choubey, "Numerical buckling analysis of graded CNT-reinforced composite sandwich shell structure under thermal loading," *Composite Structures,* vol. 216, pp. 406-414, 2019.

[52] V. Farhangi, M. Karakouzian, and M. Geertsema, "Effect of Micropiles on Clean Sand Liquefaction Risk Based on CPT and SPT," *Applied Sciences,* vol. 10, p. 3111, 2020.

[53] V. Farhangi and M. Karakouzian, "Design of Bridge Foundations Using Reinforced Micropiles," in *Proceedings of the International Road Federation Global R2T Conference & Expo, Las Vegas, NV, USA*, 2019, pp. 19-22.

[54] B. Karami, D. Shahsavari, M. Janghorban, R. Dimitri, and F. Tornabene, "Wave propagation of porous nanoshells," *Nanomaterials,* vol. 9, p. 22, 2019.

[55] M. Bakhtiari, A. Tarkashvand, and K. Daneshjou, "Plane-strain wave propagation of an impulse-excited fluid-filled functionally graded cylinder containing an internally clamped shell," *Thin-Walled Structures,* p. 106482, 2020.

[56] F. Ebrahimi and A. Seyfi, "Wave propagation response of multi-scale hybrid nanocomposite shell by considering aggregation effect of CNTs," *Mechanics Based Design of Structures and Machines,* pp. 1-22, 2019.

[57] F. Abad and J. Rouzegar, "Exact wave propagation analysis of moderately thick Levy-type plate with piezoelectric layers using spectral element method," *Thin-Walled Structures,* vol. 141, pp. 319-331, 2019.

[58] M. Habibi, M. Mohammadgholiha, and H. Safarpour, "Wave propagation characteristics of the electrically GNP-reinforced nanocomposite cylindrical shell," *Journal of the Brazilian Society of Mechanical Sciences and Engineering,* vol. 41, p. 221, 2019.

[59] C. Li, Q. Han, Z. Wang, and X. Wu, "Analysis of wave propagation in functionally graded piezoelectric composite plates reinforced with graphene platelets," *Applied Mathematical Modelling,* 2020.

[60] H. Moayedi and S. Hayati, "Applicability of a CPT-based neural network solution in predicting load-settlement responses of bored pile," *International Journal of Geomechanics,* vol. 18, 2018.

[61] H. Moayedi and S. Hayati, "Modelling and optimization of ultimate bearing capacity of strip footing near a slope by soft computing methods," *Applied Soft Computing,* vol. 66, pp. 208-219, 2018.

[62] H. Moayedi and A. Rezaei, "An artificial neural network approach for under-reamed piles subjected to uplift forces in dry sand," *Neural Computing and Applications,* vol. 31, pp. 327-336, 2019.

[63] X. Ma, L. K. Foong, A. Morasaei, A. Ghabussi, and Z. Lyu, "Swarm-based hybridizations of neural network for predicting the concrete strength," *Smart Structures and Systems,* vol. 26, pp. 241-251, 2020.

[64] K. Khorramian, S. Maleki, M. Shariati, and N. H. Ramli Sulong, "Behavior of Tilted Angle Shear Connectors (vol 10, e0144288, 2015)," *PLOS ONE,* vol. 11, 2016.

[65] M. Safa, P. A. Sari, M. Shariati, M. Suhatril, N. T. Trung, K. Wakil*, et al.*, "Development of neuro-fuzzy and neuro-bee predictive models for prediction of the safety factor of eco-protection slopes," *Physica A: Statistical Mechanics and its Applications,* p. 124046, 2020.

[66] M. Shariati, "Assessment of Building Using None-destructive Test Techniques (ultra Sonic Pulse Velocity and Schmidt Rebound Hammer)," Universiti Putra Malaysia, 2008.

[67] M. Shariati, M. S. Mafipour, P. Mehrabi, M. Ahmadi, K. Wakil, N. T. Trung*, et al.*, "Prediction of concrete strength in presence of furnace slag and fly ash using Hybrid ANN-GA (Artificial Neural Network-Genetic Algorithm)," *Smart Structures and Systems,* vol. 25, pp. 183-195, 2020.

[68] M. Shariati, A. Heyrati, Y. Zandi, H. Laka, A. Toghroli, P. Kianmehr*, et al.*, "Application of waste tire rubber aggregate in porous concrete," *Smart Structures and Systems,* vol. 24, pp. 553-566, 2019.

[69] C. Chen, L. Shi, M. Shariati, A. Toghroli, E. T. Mohamad, D. T. Bui*, et al.*, "Behavior of steel storage pallet racking connection-A review," 2019.

[70] M. Shariati, M. S. Mafipour, J. H. Haido, S. T. Yousif, A. Toghroli, N. T. Trung*, et al.*, "Identification of the most influencing parameters on the properties of corroded concrete beams using an Adaptive Neuro-Fuzzy Inference System (ANFIS)," *Steel and Composite Structures,* vol. 34, pp. 155-170, 2020.

[71] M. Safa, A. Maleka, M.-A. Arjomand, M. Khorami, and M. Shariati, "Strain rate effects on soil-geosynthetic interaction in fine-grained soil," *Geomechanics and Engineering,* vol. 19, p. 533, 2019.

[72] M. Shariati, S. M. Azar, M.-A. Arjomand, H. S. Tehrani, M. Daei, and M. Safa, "Comparison of dynamic behavior of shallow foundations based on pile and geosynthetic materials in fine-grained clayey soils," *Geomechanics and Engineering,* vol. 19, p. 473, 2019.

[73] A. Toghroli, P. Mehrabi, M. Shariati, N. T. Trung, S. Jahandari, and H. Rasekh, "Evaluating the use of recycled concrete aggregate and pozzolanic additives in fiber-reinforced pervious concrete with industrial and recycled fibers," *Construction and Building Materials,* vol. 252, p. 118997, 2020.

[74] F. Tornabene, M. Bacciocchi, N. Fantuzzi, and J. Reddy, "Multiscale approach for three-phase CNT/polymer/fiber laminated nanocomposite structures," *Polymer composites,* vol. 40, pp. E102-E126, 2019.

[75] B. Karami and D. Shahsavari, "On the forced resonant vibration analysis of functionally graded polymer composite doubly-curved nanoshells reinforced with graphene-nanoplatelets," *Computer Methods in Applied Mechanics and Engineering,* vol. 359, p. 112767, 2020.

[76] A. Wang, H. Chen, Y. Hao, and W. Zhang, "Vibration and bending behavior of functionally graded nanocomposite doubly-curved shallow shells reinforced by graphene nanoplatelets," *Results in Physics,* vol. 9, pp. 550-559, 2018.

[77] A. Ghabussi, N. Ashrafi, A. Shavalipour, A. Hosseinpour, M. Habibi, H. Moayedi*, et al.*, "Free vibration analysis of an electro-elastic GPLRC cylindrical shell surrounded by viscoelastic foundation using modified length-couple stress parameter," *Mechanics Based Design of Structures and Machines,* pp. 1-25, 2019.

[78] A. Shokrgozar, A. Ghabussi, F. Ebrahimi, M. Habibi, and H. Safarpour, "Viscoelastic dynamics and static responses of a graphene nanoplatelets-reinforced composite cylindrical microshell," *Mechanics Based Design of Structures and Machines,* pp. 1-28, 2020.

[79] H. Moayedi, R. Darabi, A. Ghabussi, M. Habibi, and L. K. Foong, "Weld orientation effects on the formability of tailor welded thin steel sheets," *Thin-Walled Structures,* vol. 149, p. 106669, 2020.

[80] A. Shariati, A. Ghabussi, M. Habibi, H. Safarpour, M. Safarpour, A. Tounsi*, et al.*, "Extremely large oscillation and nonlinear frequency of a multi-scale hybrid disk resting on nonlinear elastic foundation," *Thin-Walled Structures,* vol. 154, p. 106840, 2020.

[81] K. Jermsittiparsert, A. Ghabussi, A. Forooghi, A. Shavalipour, M. Habibi, D. won Jung*, et al.*, "Critical voltage, thermal buckling and frequency characteristics of a thermally affected GPL reinforced composite microdisk covered with piezoelectric actuator," *Mechanics Based Design of Structures and Machines,* pp. 1-23, 2020.
[82] J. N. Reddy, *Mechanics of laminated composite plates and shells: theory and analysis*: CRC press, 2003.
[83] M. Karimiasl, F. Ebrahimi, and M. Vinyas, "Nonlinear vibration analysis of multiscale doubly curved piezoelectric composite shell in hygrothermal environment," *Journal of Intelligent Material Systems and Structures,* vol. 30, pp. 1594-1609, 2019.
[84] M. Habibi, A. Mohammadi, H. Safarpour, A. Shavalipour, and M. Ghadiri, "Wave propagation analysis of the laminated cylindrical nanoshell coupled with a piezoelectric actuator," *Mechanics Based Design of Structures and Machines,* pp. 1-19, 2019.
[85] F. Ebrahimi and A. Dabbagh, "Vibration analysis of multi-scale hybrid nanocomposite plates based on a Halpin-Tsai homogenization model," *Composites Part B: Engineering,* vol. 173, p. 106955, 2019.
[86] N. Wattanasakulpong and A. Chaikittiratana, "Exact solutions for static and dynamic analyses of carbon nanotube-reinforced composite plates with Pasternak elastic foundation," *Applied Mathematical Modelling,* vol. 39, pp. 5459-5472, 2015.
[87] A. Khdeir, "Free vibration and buckling of symmetric cross-ply laminated plates by an exact method," *Journal of sound and vibration,* vol. 126, pp. 447-461, 1988.
[88] T. I. Thinh, M. C. Nguyen, and D. G. Ninh, "Dynamic stiffness formulation for vibration analysis of thick composite plates resting on non-homogenous foundations," *Composite Structures,* vol. 108, pp. 684-695, 2014.
[89] M. Safarpour, F. Ebrahimi, M. Habibi, and H. Safarpour, "On the nonlinear dynamics of a multi-scale hybrid nanocomposite disk," *Engineering with Computers,* pp. 1-20, 2020.

Author Statements:

M.S.H. Al-Furjan, Dong Won Jung, and Mostafa Habibi conceived of the presented idea.

Mohammad Amin Oyarhossein, Mostafa Habibi, Dong Won Jung, and Hamed Safarpour developed the theory and size-dependent formulations.

Hamed Safarpour, Mostafa Habibi, M.S.H. Al-Furjan, and Abdelouahed Tounsi performed the computations and numerical calculations.

All authors discussed the results and contributed to the final manuscript.

M.S.H. Al-Furjan, Mohammad Amin Oyarhossein, Hamed Safarpour, and Abdelouahed Tounsi wrote the manuscript text and formulations.

Mohammad Amin Oyarhossein, Dong Won Jung, and M.S.H. Al-Furjan answered to the reviewers' comments.